Hydrovolcanic tuff rings and cones as indicators for phreatomagmatic explosive eruptions on Mars

P. Brož[1,2] and E. Hauber[3]

Received 1 February 2013; revised 31 July 2013; accepted 2 August 2013.

[1] Hydrovolcanism is a common natural phenomenon on Earth and should be common on Mars, too, since its surface shows widespread evidence for volcanism and near-surface water. We investigate fields of pitted cones in the Nephentes/Amenthes region at the southern margin of the ancient impact basin, Utopia, which were previously interpreted as mud volcanoes. The cone fields contain pitted and breached cones with associated outgoing flow-like landforms. Based on stratigraphic relations, we determined a Hesperian or younger model age. We test the hypothesis of a (hydro)volcanic origin. Based on a detailed morphological and morphometrical analysis and an analysis of the regional context, an igneous volcanic origin of these cones as hydrovolcanic edifices produced by phreatomagmatic eruptions is plausible. Several lines of evidence suggest the existence of subsurface water ice. The pitted cones display well-developed wide central craters with floor elevations below the preeruptive surface. Their morphometry and the overall appearance are analogous to terrestrial tuff cones and tuff rings. Mounds that are also observed in the same region resemble terrestrial lava domes. The hydrovolcanic interaction between ascending magma and subsurface water and/or water ice may explain the formation of the pitted cones, although other scenarios such as mud volcanism cannot be ruled out. Together with the mounds, the cones might represent effusive and explosive edifices of a monogenetic volcanic field composed of lava domes, tuff rings, tuff cones, and possibly maars.

Citation: Brož, P., and E. Hauber (2013), Hydrovolcanic tuff rings and cones as indicators for phreatomagmatic explosive eruptions on Mars, *J. Geophys. Res. Planets*, *118*, doi:10.1002/jgre.20120.

1. Introduction

[2] Mars was volcanically active throughout most, if not all, of its history [e.g., *Werner*, 2009; *Hauber et al*., 2011; *Robbins et al*., 2011; *Xiao et al*., 2012], and volcanism played a significant role in the formation of its surface. Most volcanoes on Mars have been interpreted to be formed predominantly by effusive eruptions [*Greeley*, 1973; *Carr et al*., 1977; *Greeley and Spudis*, 1981]. Another significant factor modifying the Martian surface is water, both in liquid and frozen state, and at and beneath the surface [e.g., *Baker*, 2001; *Feldman et al*., 2004; *Smith et al*., 2009]. Therefore, interactions of magma with water and/or ice should be common on Mars. On Earth, such interactions are known to trigger hydrovolcanism [*Sheridan and Wohletz*, 1983], the natural phenomenon of magma or magmatic heat interacting with an external water source [*Sheridan and Wohletz*, 1983]. This interaction might lead to explosive, phreatomagmatic eruptions [*Lorenz*, 1987; *Morrissey et al*., 1999]. Hydrovolcanism is a common phenomenon occurring on Earth in all volcanic settings [*Sheridan and Wohletz*, 1983].

[3] The relative importance of explosive volcanism on Mars was predicted based on theoretical considerations [e.g., *Wilson and Head*, 1994, 2004]. Basically, there are two possibilities how explosive eruptions originate and how magma might be fragmented. One can be considered as a "dry" process, in which the eruption is driven solely by gases originally dissolved in the magma. It occurs when magma ascends rapidly and is accompanied by rapid decompression [*Cashman et al*., 1999]. The second possibility involves "wet" (phreatomagmatic) eruptions and occurs when magma of all types is mixed with an external water source, e.g., groundwater, ground ice [*Cashman et al*., 1999], or a surficial body of water [*Sheridan and Wohletz*, 1983]. The basic principle of this interaction is rapid heat transport from magma to water, leading to water vaporization, steam expansion and pressure buildup, and fragmentation and explosion [*Basaltic Volcanism Study Project*, 1981, p. 729]. These types of eruptions are characterized by the production of steam and fragmented magma ejected from the central vent in a series of eruptive pulses [*Sheridan and Wohletz*, 1983].

[4] Recently, several studies reported evidence of explosive volcanism forming small pyroclastic cones on Mars [*Bleacher et al*., 2007; *Keszthelyi et al*., 2008; *Brož and Hauber*, 2012], but these edifices were observed in relatively

Additional supporting information may be found in the online version of this article.

[1]Institute of Geophysics ASCR, v.v.i., Prague, Czech Republic.
[2]Institute of Petrology and Structural Geology, Faculty of Science, Charles University, Prague, Czech Republic.
[3]Institute of Planetary Research, DLR, Berlin, Germany.

Corresponding author: P. Brož, Institute of Geophysics, Institute of Geophysics ASCR, v.v.i., Boční II/1401, Prague 4, 14131, Czech Republic. (Petr.broz@ig.cas.cz)

2169-9097/13/10.1002/jgre.20120

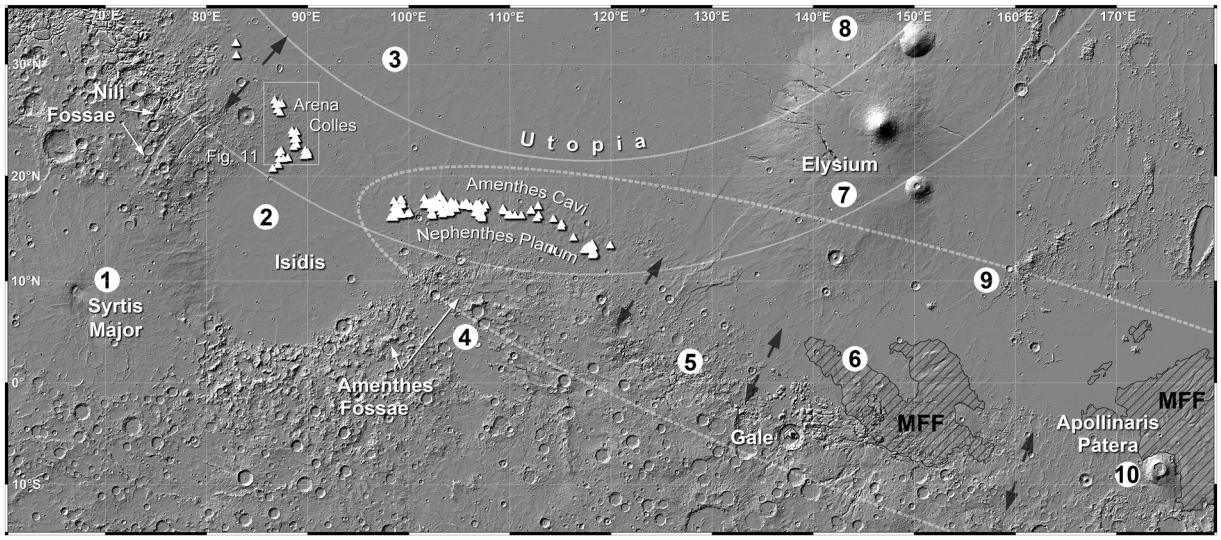

Figure 1. Study area (with pitted cones marked as white symbols) in regional context with most significant features highlighted. Large circles drawn with white lines mark perimeters of Utopia rings following *Skinner and Tanaka* [2007]. White box marks location of Figure 11, black arrows mark extension as reported by *Watters* [2003]. White ellipse (dashed line) shows hypothetical dispersal of volcanic ash from the NAC cone field, indicating a possible contribution to the Medusae Fossae Formation. 1 - Low-relief shield volcano Syrtis Major, 2 - Pseudocraters in Isidis Planitia [*Ghent et al*., 2012], 3 - Rift zone volcanism [*Lanz et al*., 2010], 4 - Volcanic flooding [*Erkeling et al*., 2011], 5 - Possible subglacial volcanoes [*de Pablo and Caprarelli*, 2010], 6 - Cone fields with hydrothermal activity [*Lanz and Saric*, 2009], 7 - Elysium bulge, 8 - Phreatomagmatic eruptions [*Wilson and Mouginis-Mark*, 2003a], 9 - Cerberus Fossae and Athabasca Valles [e.g., *Plescia*, 2003] and 10 - Apollinaris Patera.

"dry" environments (i.e., in Tharsis, for example at Pavonis Mons, Mareotis Tholus, Ulysses Fossae), and hence the explosive eruptions were probably driven by magma degassing. Only *Meresse et al*. [2008] and *Lanz et al*. [2010] investigated areas with pyroclastic cones that might have experienced a higher abundance of water/water ice. *Meresse et al*. [2008] focused on Hydraotes Chaos, a region thought to have formed by volcanic interaction with a subsurface layer enriched in water ice. *Meresse et al*. [2008] proposed that the formation of volcanic sills caused melting of the ice and the release of the water at the surface. On the other hand, *Lanz et al*. [2010] investigated pyroclastic cones associated with a rift-like structure in Utopia Planitia, an area that may have been enriched in water ice, too [*Erkeling et al*., 2012]. It is now clear that water ice is common in the shallow Martian subsurface at a wide range of latitudes [e.g., *Feldman et al*., 2004; *Smith et al*., 2009; *Byrne et al*., 2009; *Vincendon et al*., 2010]. Thus, it is reasonable to expect that phreatomagmatic explosions left some observable evidence [*Carruthers and McGill*, 1998]. Indeed, several in situ observations made by rovers suggest the past action of hydrovolcanic explosions [e.g., *Rice et al*., 2006; *Schmidt et al*., 2006; *Ennis et al*., 2007; *Keszthelyi et al*., 2010] and other studies based on remote sensing data suggested phreatomagmatic activity [e.g., *Wilson and Mouginis-Mark*, 2003a, 2003b; *Wilson and Head*, 2004]. Despite the growing evidence of Martian volcanic diversity, the most abundant hydrovolcanic landforms on Earth, i.e., tuff rings, tuff cones, and maars [*Sheridan and Wohletz*, 1983], were not yet reported in detail from Mars [*Keszthelyi et al*., 2010].

[5] Here we present our observations of a large field of pitted cones along the dichotomy boundary in the Nephentes Planum and Amenthes Cavi region (Figure 1), previously interpreted by *Skinner and Tanaka* [2007] as mud volcanoes. In the following, we refer to these cones as the Nephentes-Amenthes Cones (NAC). For the first time, we also report observations of another cone field north of Isidis Planitia in the Arena Colles region, which was previously unknown. This field is located in an almost identical geotectonic context, at a topographic bench along the margin of Utopia. Previous studies of the NAC are sparse. They were briefly mentioned by *Erkeling et al*. [2011], who referred to them as "volcano-like landforms" without further explanation. To our knowledge, the only in-depth study is that of *Skinner and Tanaka* [2007], who interpreted these cones as mud volcanoes. This conclusion was based on the morphological analysis of an assemblage of landforms which consists of four elements: (1) fractured rises, (2) mounds, (3) isolated and coalesced depressions, and (4) the pitted cones which are the main subject of our study. *Skinner and Tanaka* [2007] considered the tectonic and sedimentary setting of the NAC and compared the landforms to possible terrestrial analogues. They developed a consistent scenario of mud volcanism that considers the local morphology as well as the regional tectonic context. According to their hypothesis, the giant Utopia impact formed a multiring basin [e.g., *Spudis*, 1993]. Deposits filled and loaded the central part of the basin, whereas parts of the periphery were partly eroded and relaxed, producing an overall gently sloping basin surface. *Skinner and Tanaka* [2007] hypothesized that volatile-rich components were sedimented in annular ring grabens. These buried regions of weekly consolidated material enabled the formation of weaker zones beneath surface, which serve as a source reservoir for sedimentary diapirism. Material could have been mobilized

through processes such as density inversion, seismicity, or contractional tectonism as implied by wrinkle ridges. Each mobilization would have led to resurfacing by mud effusion forming pitted cones, mud flows, and mounds. As a result of mud volcanism, in which fine-grained material from deeper crustal levels would have moved upward to the surface, the Amenthes Cavi were then formed by subsidence in response to the source region depletion.

[6] It is not our objective to disprove the mud volcano hypothesis of *Skinner and Tanaka* [2007], which offers a self-consistent scenario for landscape modification of the NAC region in the Hesperian. Instead, our aim is to test the alternative hypothesis of an igneous volcanic origin of the pitted cones and mounds. We compare the NAC with terrestrial analogues, both of igneous and mud volcanic origin, and discuss the most significant discrepancies and consistencies. We show that morphologically analogous structure may be found elsewhere on Mars, suggesting that the NAC may not be unique on Mars and therefore may not require a unique geologic context for their formation. Finally, we explore scenarios that may explain igneous volcanism at the study area.

2. Data and Methods

2.1. Images and Topography

[7] For morphological analyses, we used different image data sets acquired by several cameras, i.e., Context Camera (CTX) [*Malin et al*., 2007], High Resolution Stereo Camera (HRSC) [*Jaumann et al*., 2007], and High Resolution Imaging Science Experiment (HiRISE) [*McEwen et al*., 2007], with typical resolutions of 5–6 m/pixel, 10–20 m/pixel, and ~30 cm/pixel, respectively. CTX and HRSC image data were processed by the USGS Astrogeology image processing software, Integrated System for Imagers and Spectrometers (ISIS3), and Video Imaging Communication and Retrieval (VICAR), respectively.

[8] Topographic information (e.g., elevations and slope angles) was derived from gridded Digital Elevation Models (DEM) derived from stereo images (HRSC). HRSC DEM are interpolated from 3D points with an average intersection error of 12.6 m and have a regular grid spacing of 50 to 100 m [*Scholten et al*., 2005; *Gwinner et al*., 2009]. Although is well known that the quantification of various morphometric parameters depends on DEM resolution [e.g., *Kienzle*, 2004; *Guth*, 2006], even coarse DEM with a resolution equal or lower than HRSC DEM (e.g., DEM derived from Shuttle Radar Topography Mission (SRTM) with a grid size of typically 90 m) can be used for reliable measurements of volcano topography [*Wright et al*., 2006; *Gilichinsky et al*., 2010]. Importantly, the size of the investigated feature should be several times larger than the spatial DEM cell size [*Kervyn et al*., 2007]. The investigated NAC cones have typical basal diameters of >5 km and are therefore about two orders of magnitude larger than HRSC DEM grid sizes. Hence, the main results of our topographic analyses should be robust, although it cannot be excluded that flank slopes derived from HRSC DEM somewhat underestimate the true maximum flank slopes.

[9] For comparative analyses, terrestrial data were obtained from Google Earth software [*Google Inc*., 2011]. Google Earth uses DEM data collected by NASA's Shuttle Radar Topography Mission [*Farr et al*., 2007] with a cell size of 10 to 30 m for the USA, and around 90 m for the rest of the world (the case of Azerbaijan). The vertical error of these DEM is reported to be less than 16 m [*Jarvis et al*., 2008]. It has to be noted, however, that using this data may raise some problems. These are caused by the 90 m SRTM DEM, which is not ideal for small-scale (500 m) and/or steep topographic features [*Kervyn et al*., 2008], because it might lead to some measurement uncertainties. On the other hand, similar uncertainties are possibly associated with data from Mars used for morphometric comparison.

2.2. Cluster Analysis: Nearest Neighbor and Two-Point Azimuthal Analysis

[10] To analyze the spatial distribution of cones within the field of NAC, we used Average Nearest Neighbor, part of Spatial Statistics tool in ArcGIS 10. This tool enables determination of clustering or dispersing behavior of investigated features by measuring the distance from every point (i.e., surface feature) to its nearest neighbor. The method is based on testing the randomness in spatial distribution by calculating the ratio between the observed mean distance and the expected mean distance for a random point distribution. If the ratio is <1, the points are clustered; the closer to zero, the more clustered [*Clark and Evans*, 1954].

[11] The two-point azimuth technique developed by *Lutz* [1986] can be used to identify structurally controlled trends within a volcanic field. It tests if there is a preferential alignment of points along certain orientations [*Cebriá et al*., 2011]. This method is based on a quantitative analysis of the azimuth angles of lines connecting each vent with all other vents, thus connecting all possible pairs of points in the investigated area (for N points, the total number of lines is N(N−1)/2). A vent is represented by a discrete point [*Cebriá et al*., 2011] and can therefore be used for this technique. The method was tested in different terrestrial and Martian volcanic fields [e.g., *Wadge and Cross*, 1988; *Connor*, 1990, *Lutz and Gutmann*, 1995; *Bleacher et al*., 2009; *Richardson et al*., 2013]. A modification of the two-point azimuth technique was developed by *Cebriá et al*. [2011], who defined a minimum significant distance between vents (equation (1)) to eliminate potential problems with a preferential alignment of points caused by the shape of the investigated area.

$$d = \leq \frac{(x\text{-}1\sigma)}{3} \tag{1}$$

where d is the minimum significant distance, x is the mean of all distances between vents, and σ is the standard deviation of the mean distance between vents. This minimum significant distance should be able to filter out any large amount of non-significant data corresponding to the most likely orientation caused by the shape of the investigated area [*Cebriá et al*., 2011]. For example, a field in the shape of a narrow ellipse will lead to a preferred orientation in the direction of the semimajor axis of the ellipse. This is exactly the case of the NAC field, which is elongated in an east-west direction. A histogram of azimuth values (from 0° = north, 90° = east, 180° = south) was produced, with bins of 15°. Following earlier authors [*Lutz*, 1986; *Bleacher et al*., 2009; *Cebriá et al*., 2011], we expect that bins containing an anomalously high number of lines connecting vents are evidence for a structural relationship or alignment between vents in the field.

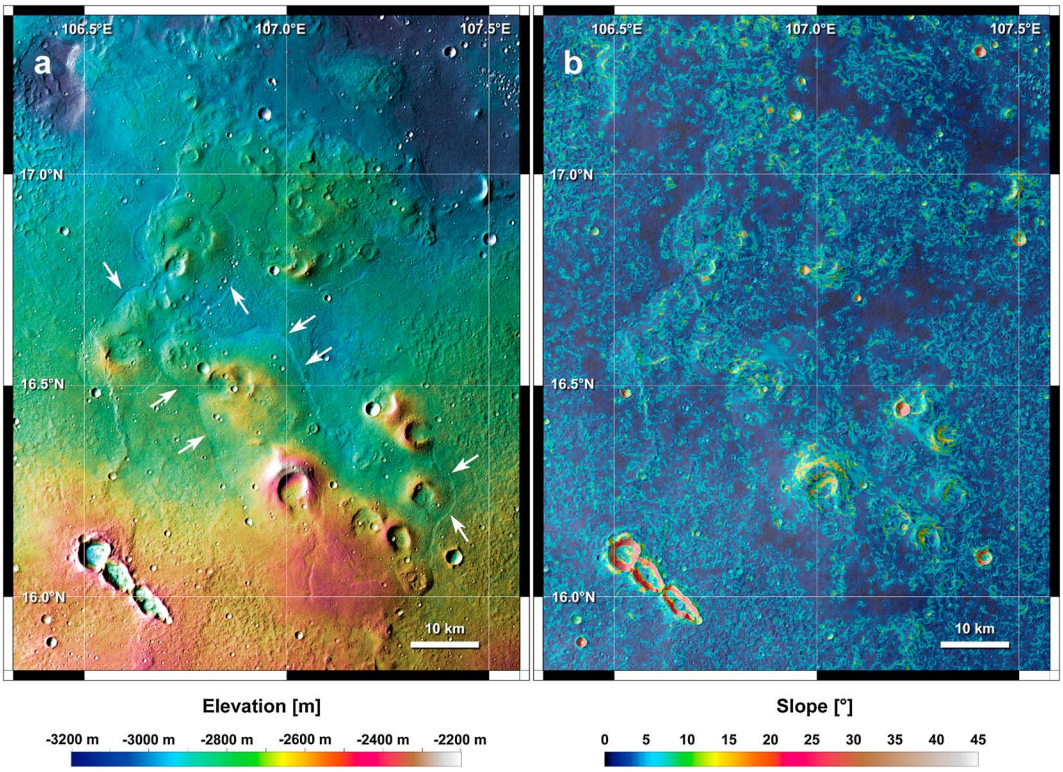

Figure 2. Pitted cones in the NAC field. (a) Topographic image map. Note the clustered distribution and the fact that several of the cones are breached in different directions. Smooth lobate material embays the cones (arrows). Detail of HRSC imaging sequence h3032_0000, orthoimage overlain by color-coded DEM derived from stereo images. (b) Slope map derived from HRSC DEM. Slopes were measured over a baselength of 50 m, corresponding to the cell size of the HRSC DEM.

[12] To get information about morphological parameters and distinguish between different classes of volcanic edifices, we used three main morphometrical parameters already widely used by several authors in a range of terrestrial and Martian volcanic fields [e.g., *Porter*, 1972; *Wood*, 1980; *Brož and Hauber*, 2012; *Kervyn et al*., 2012]. Specifically, cone diameter (W_{CO}) and crater diameter (W_{CR}) were determined by averaging two measurements in different directions. Cone height (H_{CO}) and crater depth (D_{CR}) were obtained from HRSC DEM. These basic parameters were used to calculate three basic ratios, W_{CR}/W_{CO}, H_{CO}/W_{CO}, and H_{CO}/W_{CR}. To enable comparison of data from different sources, we used crater depth (D_{CR}) as the difference between the mean crater rim elevation and the lowest observed elevation inside the crater as used by *Kervyn et al*. [2012].

2.3. Ages

[13] The absolute cratering model age determination of planetary surfaces uses the crater size-frequency distribution as measured on images [*Crater Analysis Techniques Working Group*, 1979]. Representative surface areas for age determinations are mapped on the basis of morphology (stratigraphy), and craters were counted on CTX images utilizing the software "cratertools" [*Kneissl et al*., 2011]. Absolute cratering model ages were derived with the software tool "craterstats" [*Michael and Neukum*, 2010] by analysis of the crater-size frequency distributions applying the production function coefficients of *Ivanov* [2001] and the impact cratering chronology model coefficients of *Hartmann and Neukum* [2001].

3. Regional Setting

[14] The study area lies close to the dichotomy boundary, between cratered highlands of Tyrrhena Terra in the south and smoother appearing plains of Utopia Planitia in the north (Figure 1). It is located on a topographic bench termed Nephentes Planum and also contains part of the Amenthes Cavi region (10°N to 20°N and 95°E to 125°E). The regional context was described by *Tanaka et al*. [2003, 2005] and *Skinner and Tanaka* [2007] and mentioned by *Erkeling et al*. [2011]. The whole NAC region is covered by dust, which complicates identifying surface details. Utopia Planitia probably formed by a giant impact during the pre-Noachian period around 4.5–4.1 Ga [e.g., *McGill*, 1989; *Tanaka et al*., 2005; *Carr and Head*, 2010]. In an extension of McGill's original basin interpretation for Utopia [*McGill*, 1989], *Skinner and Tanaka* [2007] proposed the existence of annular ring basins that would have acted as locations of sediment accumulation in southern Utopia Planitia. Another relatively close basin is Isidis Planitia [e.g., *Schultz and Frey*, 1990], lying west of the Nephentes/Amenthes region and contributing to the history of the western part of the study area [*Erkeling et al*., 2011]. Close to the rim of Isidis Planitia, near the southern part of the investigated area, a series of NNE trending tectonic grabens, Amenthes Fossae, indicate extensional tectonics associated with the Isidis impact [*Erkeling*

et al., 2011], analogous to the morphologically similar graben system, Nili Fossae, to the NW of Isidis. Isidis was formed later than Utopia [*Tanaka et al*., 2005]. *Ivanov et al*. [2012] interpreted the area of Isidis Planitia as a volcanic center which was mainly active at ~3.8–3.5 Ga. Later, the area experienced fluvial/glacial activity (early Hesperian-early Amazonian, ~3.5–2.8 Ga), and the associated processes may have left wet deposits on the floor of Isidis [*Ivanov et al*., 2012].

[15] The region hosting the NAC is bordered to the East by the Elysium bulge and Elysium Planitia, previously recognized as significant volcanic centers [*Malin*, 1977; *Plescia*, 1990]. The spatially closer regional context displays several lines of evidence for subsurface water ice (rampart craters, pseudo-craters, and the Hephaestus and Hebrus Fossae channels). Recently, several studies reported volcanic activity at various locations in a broad area around the NAC region [*de Pablo and Pacifici*, 2008; *de Pablo and Caprarelli*, 2010; *Lanz et al*., 2010; *Ghent et al*., 2012], suggesting focused locations of potential volcanic activity in the regional context.

4. Observations

4.1. Morphology

4.1.1. Cones

[16] The study area containing the NAC displays ~170 pitted cones (on the basis of fewer and lower resolution images, *Skinner and Tanaka* [2007] had already identified ~85 cones) that are widely spread throughout the area of interest. Cones often coalesce and/or overlap each other and form chaotic clusters (Figure 2a). They display texturally smooth flanks and typically wide central craters (Figure 3). In many cases, the rims of the central craters are breached, and only segments of a full cone can be observed (Figure 4). In several cases, lobate flows seem to have emanated from breached cones and moved gravitationally downslope (see Figure 2a, marked with white arrows). Flank slopes of cones are mainly concave-upward, but can turn to convex near the crater rims. High-resolution HRSC DEMs show that flank slopes are typically below 10°, but can reach up to about 20° in the steepest parts close to the crater rim (see Figure 2b). Crater floors may have elevations above or, interestingly, below the surrounding plains (Figure 4; see Table S1 in the auxiliary material for cone heights and crater depths).

[17] The study area is not fully covered by HRSC DEM, limiting the amount of cones suitable for morphometric study to a subset of ~50 cones. Based on detailed morphological measurements, the investigated cones are ~3 to 15 km wide (mean 7.8 km; based on measurements of 92 edifices) and ~30 to ~370 m high (mean ~120 m; based on measurements of 53 edifices), resulting in an average H_{CO}/W_{CO} ratio of 0.016 (based on measurements of 52 edifices). Many cones have well-developed central deep and wide craters (average depth 80 m; based on 52 edifices; average width 3.1 km, based on measurements of 92 edifices), resulting in a large W_{CR}/W_{CO} ratio of 0.42 (for more details about all measurements see Table S.1 in the auxiliary material). These values differ in some aspects slightly from those obtained by *Skinner and Tanaka* [2007]. They reported basal cone diameters in the range of 4 to 8 km (mean 6.4 km), with heights below 300 m (mean 230 m), cone slopes between 2° and 9° (mean ~6°). However, it is not clear how many cones were measured by *Skinner and Tanaka* [2007] and which cones were selected for detailed investigations. Therefore, no direct comparison with our data was possible.

[18] *Skinner and Tanaka* [2007] used mud volcanoes in Azerbaijan as terrestrial analogues to the cones in the NAC region, but without details on their morphometry. Therefore, we also measured basic morphological parameters of cones in Azerbaijan (Table 1). The mud volcanoes have average basal widths and heights of ~4 km and ~200 m, respectively. They possess craters with an average diameter of 460 m, but since the crater depth could not be resolved in the available data, it is thought to be commonly less than 10 m. The W_{CR}/W_{CO} ratio is on average 0.13; the W_{CO}/W_{CR} and H_{CO}/W_{CO} ratios are 0.5 and 0.05, respectively. In comparison to the NAC, the mud volcanoes in Azerbaijan have a significantly lower W_{CR}/W_{CO} ratio (0.13 as compared to 0.42) and a higher H_{CO}/W_{CO} ratio (0.05 vs. 0.016). In relation to their diameters, therefore, they have smaller craters and larger heights than the NAC.

[19] In addition, we collected morphometric measurements of volcanic edifices on Mars and Earth published in earlier studies [*Pike*, 1978; *Hasenaka and Carmichael*, 1985; *Inbar and Risso*, 2001; *Hauber et al*., 2009a; *Brož and Hauber*, 2012] and compared them to the corresponding results obtained for the NAC (Table 2). The underlying substrate consists of plains material with a very low regional slope, and therefore the results should not be affected by slope effects [*Tibaldi*, 1995]. A graphical representation of the W_{CR}/W_{CO} versus W_{CO} ratio, commonly used in remote sensing-based attempts to classify volcanic edifices [e.g., *Pike*, 1978; *Hasenaka and Carmichael*, 1985; *Inbar and Risso*, 2001; *Hauber et al*., 2009a; *Brož and Hauber*, 2012], reveals that the NAC are clearly distinguished from other igneous volcanic edifices on Earth and Mars as well as from the mud volcanoes in Azerbaijan (Figure 5). Specifically, the NAC have a larger cone width than terrestrial tuff rings and maars, although the W_{CR}/W_{CO} ratio is identical. Similarly, terrestrial cinder cones are smaller in their basal diameters, with a larger spread in their W_{CR}/W_{CO} ratios. Martian cinder cones [*Brož and Hauber*, 2012] are also smaller in diameter than the NAC. On the other hand, low volcanic shields built by effusive volcanism (i.e., lava flows) have comparable basal diameters, but are distinguished from the NAC by a significantly higher W_{CR}/W_{CO} ratio. Finally, the mud volcanoes in Azerbaijan are both smaller in diameter and have lower W_{CR}/W_{CO} ratios.

4.1.2. Mounds

[20] Another type of positive topographic landform in the NAC area is represented by small mounds with subcircular to elliptical planform shapes. These features were also already described by *Skinner and Tanaka* [2007], who identified around 80 edifices predominantly distributed in the central and eastern parts of the NAC study area, forming their own clusters independently of pitted cones. Some of them, however, are situated within the clusters of pitted cones. According to *Skinner and Tanaka* [2007], the basal diameters of these mounds range from 2 to 12 km (mean 4 km), with heights between 10 and 200 m (where measurable). Many mounds have small summit cones or pits a few hundred meters across near their centers. Mounds can be aligned along structural lineaments (Figure 6a). As for the cones, it is not clear which mounds were selected by *Skinner and*

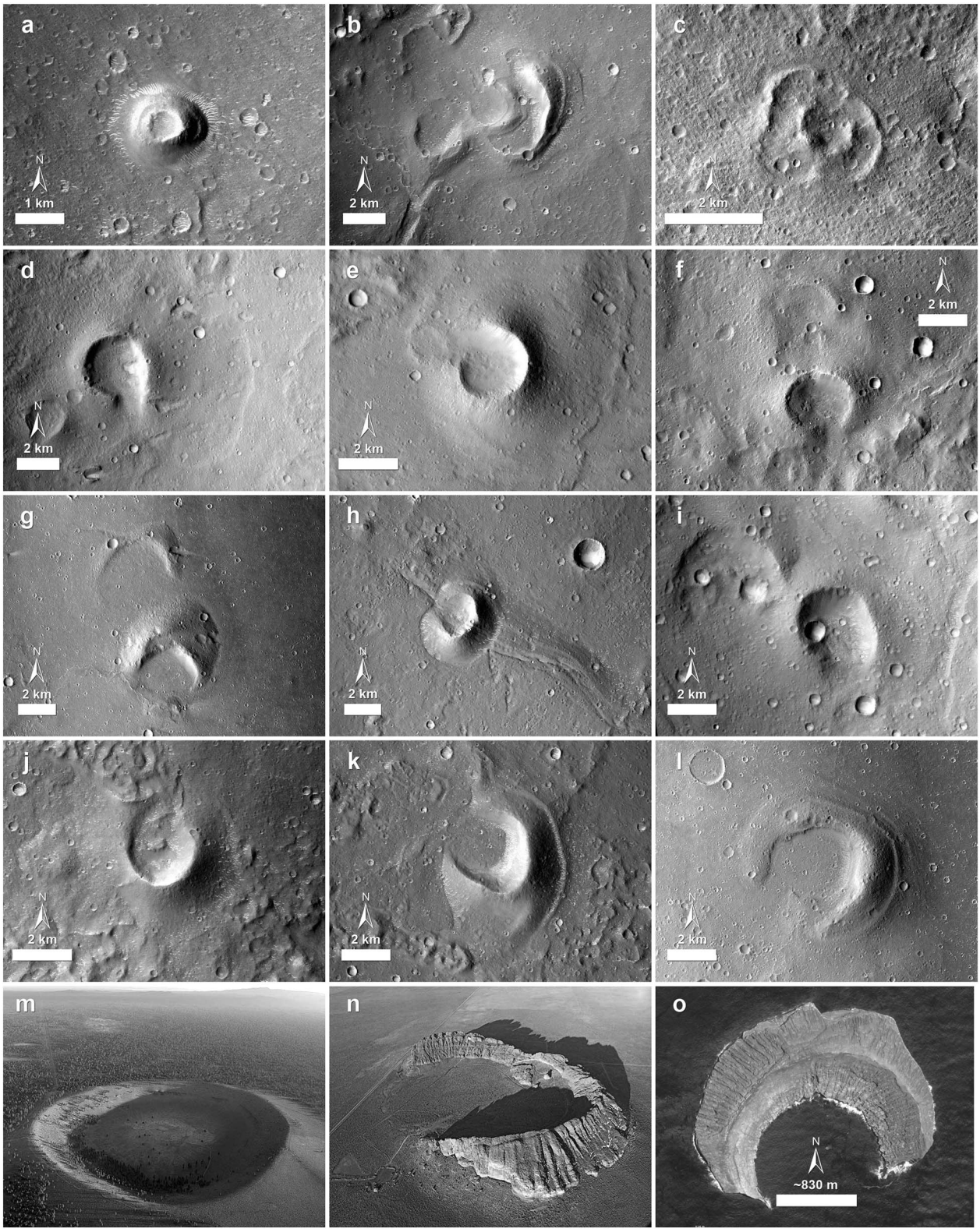

Figure 3

Tanaka [2007] for measurements and where they are situated. *Skinner and Tanaka* [2007] also noted that mounds are often situated proximal or on top of wrinkle ridges or large arches. Our observations confirm the reports of *Skinner and Tanaka* [2007] on the distribution and general properties of these mounds, especially the existence of the small central hills (see Figure 6b).

4.1.3. Other Morphological Features

[21] In several cases, we observed flow-like features emanating from the central vents of cones, which had already

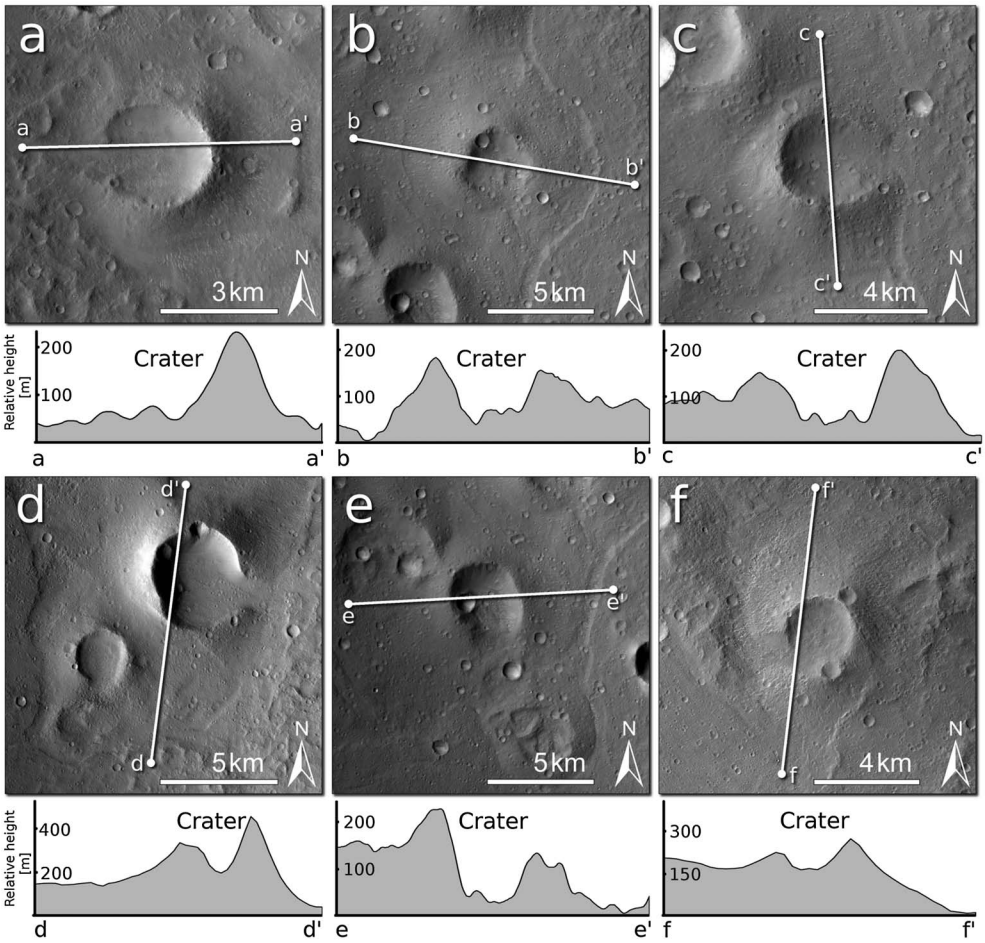

Figure 4. Details of several investigated cones in the NAC field. Note the wide central craters with floor elevations sometimes below surrounding surface level (image a = cone B15, CTX P17_007489_1967; image b = cone C28, CTX G01_018499_1961; image c = cone C27, CTX G01_018499_1961; d = cone B35, CTX P04_002452_1969; e = cone C30, CTX G01_018499_1961; f = cone B68, CTX B19_017075_1974). For locations, see Table S.1 in the auxiliary material.

been identified and described by *Skinner and Tanaka* [2007]. Elsewhere, small-scale morphological details (Figure 7a) revealed by the inspection of HiRISE images do not provide unambiguous evidence for one or the other formation mechanism. The flanks of one pitted cone (Figure 7b) are cut by fractures arranged in a polygonal pattern (Figure 7c), which resembles desiccation cracks and would be consistent with tensional stresses acting on a drying mud surface [e.g., *Konrad and Ayad*, 1987]. The fractured material may have formed much later as a mantling deposit and may not be directly associated with the origin of the cone. On the other hand, small-scale impacts into the flanks of this cone excavated

Figure 3. Examples of pitted cones in the NAC field and examples of terrestrial tuff rings for comparison. (a) Cone at 16°N/114.56°E. This cone is unusual in that its crater rim is not breached (detail of CTX G01_018657_1961). (b) Nested cones near 16.97°N/112.30°E; detail of CTX P22_009519_1969. (c) Cone with nested craters at 17.6°N/104.57°E; detail of CTX B19_017075_1974. (d) Two cones near 16.5°N/102.37°E; detail of CTX P17_007489_1967. (e) Cone at 16.62°N/103.33°E; detail of CTX P04_002452_1969. (f) Cone at 16.67°N/104.13°E; detail of CTX G01_018776_1974. (g) Two cones, one of them only with a remaining small segment, near 18.31°N/103.11°E; detail of CTX P04_002452_1969. (h) Cone aligned along and split by a fissure, centered at 16.49°N/111.31°E; detail of CTX G04_019857_1964. (i) Two cones at 16.16°N/107.25°E (detail of CTX G01_018499_1961). (j) Cone at 16.05°N/112.86°E; detail of CTX P21_009308_1962. (k) Prominent cone at 16.48°N/113.07°E; detail of CTX B03_010653_1966. Note the morphological similarity to the terrestrial tuff ring, Fort Rock (Oregon, USA), in Figure 3n. (l) Cone at 17.06°N/104.19°E; CTX mosaic of B19_017075_1974 and G01_018776_1974. Note the morphological similarity to the tuff ring on the Galápagos Islands (Ecuador) in panel Figure 3o. (m) Maar "Hole-in-the-Ground" (Oregon, USA; rim-to-rim diameter ~1500 m; oblique view toward NW; image: Q. Myers). Note similarity to Figures 3d, 3e, 3f, and 3j. (n) Tuff ring "Fort Rock" (Oregon, USA; diameter ~1300 m, oblique view toward WSW; image: Q. Myers). Note similarity to Figure 3k. (o) Tuff ring on the Galápagos Islands (Ecuador; image: DigitalGlobe, obtained via GoogleEarth). Note similarity to Figure 3l.

Table 1. Measurement of Mud Volcanoes in Azerbaijan Used as Terrestrial Analogues by *Skinner and Tanaka* [2007][a]

ID	Location	W_{CO} (m)	W_{CR} (m)	Height (m)	Depth of Crater (m)	W_{CR}/W_{CO}	H_{CO}/W_{CR}	H_{CO}/W_{CO}
1	40.32°N, 49.43°E	2782	950	130	non	0.34	0.14	0.05
2	40.32°N, 49.31°E	3050	610	127	non	0.20	0.21	0.04
3	40.27°N, 49.30°E	1880	250	119	non	0.13	0.48	0.06
4	40.26°N, 49.31°E	2540	180	138	non	0.07	0.77	0.05
5	40.22°N, 49.35°E	3300	260	142	non	0.08	0.55	0.04
6	40.16°N, 49.30°E	4980	580	280	non	0.12	0.48	0.06
7	40.14°N, 49.38°E	4600	450	380	non	0.10	0.84	0.08
8	40.24°N, 49.51°E	6200	815	291	non	0.13	0.36	0.05
9	40.38°N, 49.61°E	3350	380	228	non	0.11	0.60	0.07
10	40.02°N, 49.37°E	3300	400	160	non	0.12	0.40	0.05
11	39.97°N, 49.36°E,	3170	210	198	non	0.07	0.94	0.06
12	39.92°N, 49.26°E	4450	750	200	non	0.17	0.27	0.04
13	40.11°N, 49.34°E	6030	430	233	non	0.07	0.54	0.04
14	40.01°N, 49.36°E	2020	438	52	19	0.22	0.12	0.03
15	40.15°N, 49.18°E	2200	336	165	non	0.15	0.49	0.08
17	40.01°N, 49.25°E	5250	320	281	non	0.06	0.88	0.05
Average	Location	3694	460	195	non	0.13	0.50	0.05

[a]Measurements based on Google Earth software [*Google Inc*., 2011; *Jarvis et al*., 2008]. Most mud volcanoes in Azerbaijan do not show any evidence of a deep crater on their top.

boulders with sizes of several meters from the fractured material (Figures 7d and 7e). This may suggest a material with considerable cohesive strength, because it did not break apart during ejection and landing. The required strength may be easier explained by igneous volcanic material than by compacted mud.

4.1.4. Spatial Alignment

[22] We investigated the spatial alignment of cones in the study area to test if there is some structural control within the field which might explain its origin. We also tested if the cones are clustered by using the Average Nearest Neighbor tool in ArcGIS 10. If the ratio is <1, the points are statistically clustered; the closer to zero, the more clustered [*Clark and Evans*, 1954]. Our results reveal a Nearest Neighbor Ratio of 0.44, which indicates clustering. Clustering of vents is a well-known characteristic for terrestrial fields of monogenetic volcanoes [e.g., *Connor and Conway*, 2000]. However, clustering may also be a common characteristic of other landforms with similar topographic appearance [*Burr et al*., 2009]. For example, pseudocraters on Mars can be clustered when certain conditions of lava emplacement are met [*Hamilton et al*., 2011], and clustering is common for vent populations inside the crater of mud volcanoes [*Roberts et al*., 2011] and even for mud volcanoes itself [*Burr et al*., 2009].

[23] The application of the two-point azimuth technique (Figure 8) did not reveal any dominant trend (see the rose diagram in Figure 8 for details) which would indicate significant structural control. However, a weak peak in orientation is visible between 45°N and 60°N. This is quite different from the trend of the Amenthes Fossae, which are oriented between 15°N and 30°N. Therefore, we discard the possibility that the cone orientation would be controlled by a now hidden fracture set with the same orientation as the Amenthes Fossae. We were also not able to detect any link to the formation of Elysium Planitia.

[24] The NAC area contains numerous wrinkle ridges, which are contractional tectonic features with positive relief, commonly interpreted as thrust-propagation folds [*Mueller and Golombek*, 2004]. Most of them have an orientation between 10°N and 20°N in the area of pitted cones and mounds [*Head et al*., 2002]. There is no obvious correlation between the results of the two-point azimuth technique and the dominant wrinkle ridge trend.

4.2. Chronology

[25] Small clusters of pitted cones do not represent suitable areas for the determination crater size-frequency distributions because they are small, relatively steep (specifically in the crater areas) and typically heavily affected by secondary

Table 2. Morphometric Comparison of Terrestrial and Martian Landforms That Resemble Tuff Cones and Tuff Rings

Volcanic Field or Region	Type	N	W_{CO} (m)	W_{CR} (m)	H_{CO} (m)	Depth of Crater (m)	W_{CR}/W_{CO}	H_{CO}/W_{CR}	H_{CO}/W_{CO}	Source
Azerbaijan	mud volcanoes	16	3694	460	195	none	0.13	0.50	0.05	This study[a]
Xalapa (Mexico)	cinder cones	57	698	214	90	none	0.32	0.42	0.13	*Rodriguez et al*. [2010]
Ulysses Colles, Mars	cinder cones	29	2300	620	230	none	0.28	0.37	0.13	*Brož and Hauber* [2012]
La Caldera de Montana Blanca, Lanzarote	tuff cone	1	1555	1106	109	191	0.71	0.10	0.07	*Kervyn et al*. [2012]
Crater Elegante, Mexico	tuff ring	1	3350[a]	1600	50	200	0.48	0.03	0.01	*Wohletz and Sheridan* [1983]
Kilbourne Hole, New Mexico	tuff ring	1	5600[a]	2500	50	80	0.45	0.02	0.01	*Wohletz and Sheridan* [1983]
Cone B39, Amenthes Region, Mars	tuff ring (?)	1	7675	3185	227	220	0.41	0.07	0.03	This study[b]

[a]Based on Google Earth, this study.
[b]Based on HRSC DEM and CTX image.

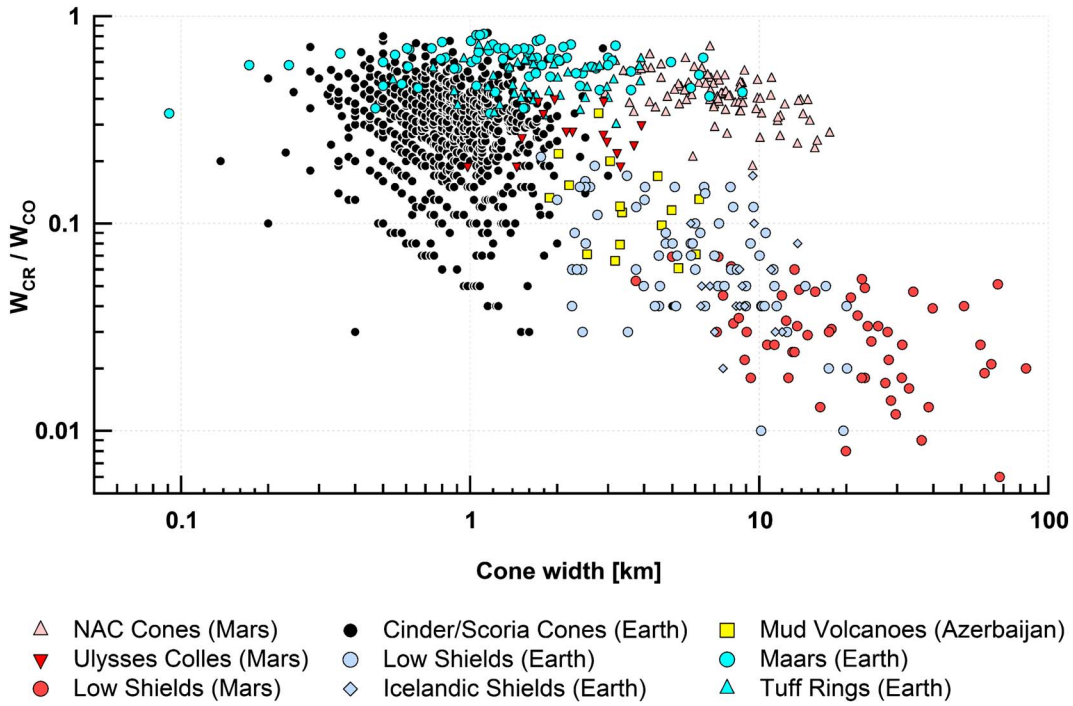

Figure 5. Morphology of pitted cones in Amenthes region in comparison with several other types of terrestrial and martian volcanic cones displayed in plot of the ratio W_{CR}/W_{CO} versus the basal width (W_{CO}). Data for investigated cones in Amenthes are from Table S.1 in the auxiliary material, for terrestrial mud volcanoes in Azerbaijan from Table 1 based on Google Earth observations, values for martian low shield volcanoes from *Hauber et al*. [2009b], for martian cinder cones (Ulysses Colles) from *Brož and Hauber* [2012], for tuff rings and maars from *Pike* [1978] and for terrestrial cinder cones from *Hasenaka and Carmichael* [1985], *Pike* [1978] and *Inbar and Risso* [2001]. Note the difference in position and therefore W_{CR}/W_{CO} ratio between the NAC pitted cones and mud volcanoes that were offered as analogues by *Skinner and Tanaka* [2007].

craters. All these factors would lead to considerable uncertainties of absolute model ages. Instead, we made use of the relative stratigraphy between the ejecta blankets of rampart craters and pitted cones. In some cases, rampart ejecta are partly overlapping or embaying pitted cones, indicating that at least some of these cones must be older than the associated impact. We choose one representative case where the stratigraphic relation is obvious and where the ejecta blanket does not exhibit clusters of secondary craters. We determined an absolute model age of ~2.4 Ga (see Figure 9 for more details), which implies that at least some of the activity producing the pitted cones has to be older than that. The maximum age of the landforms is poorly constrained.

[26] We estimate a Hesperian or younger age for the modification of the plains that host the cones, an age that would be consistent with *Skinner and Tanaka*'s [2007] age estimate. The relatively smooth flanks of the cones, which do not show evidence of fluvial dissection, also point to a formation time

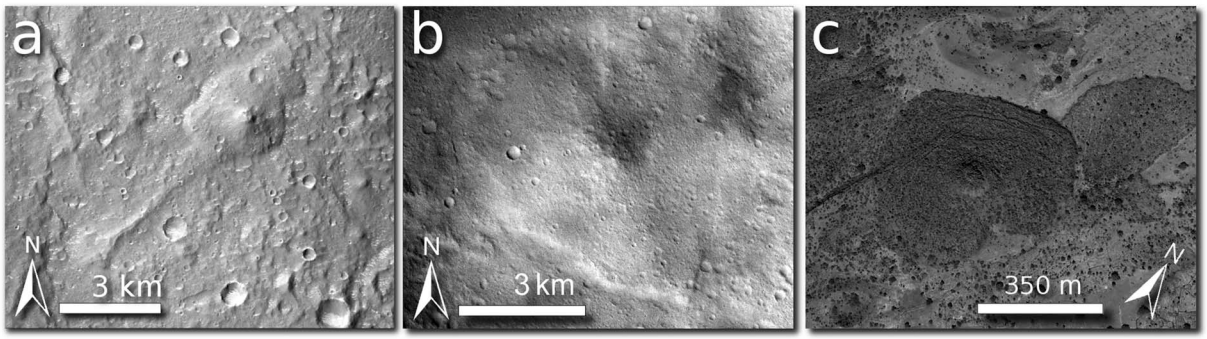

Figure 6. (a) Mound aligned along a NE trending structural feature (at 16.5°N/112.79°E; detail of CTX image P21_009308_1962). (b) Example of mound in NAC field with small central hill surrounded by outgoing material (image centered at 16.85°N/103.52°E; detail of CTX image B11_013963_1975). (c) Morphologically analogous lava dome [e.g., *Buisson and Merle*, 2002]. The image shows coulées in a volcanic field on the northern side of Tullu Moje in Ethiopia (image: GeoEye, obtained via GoogleEarth).

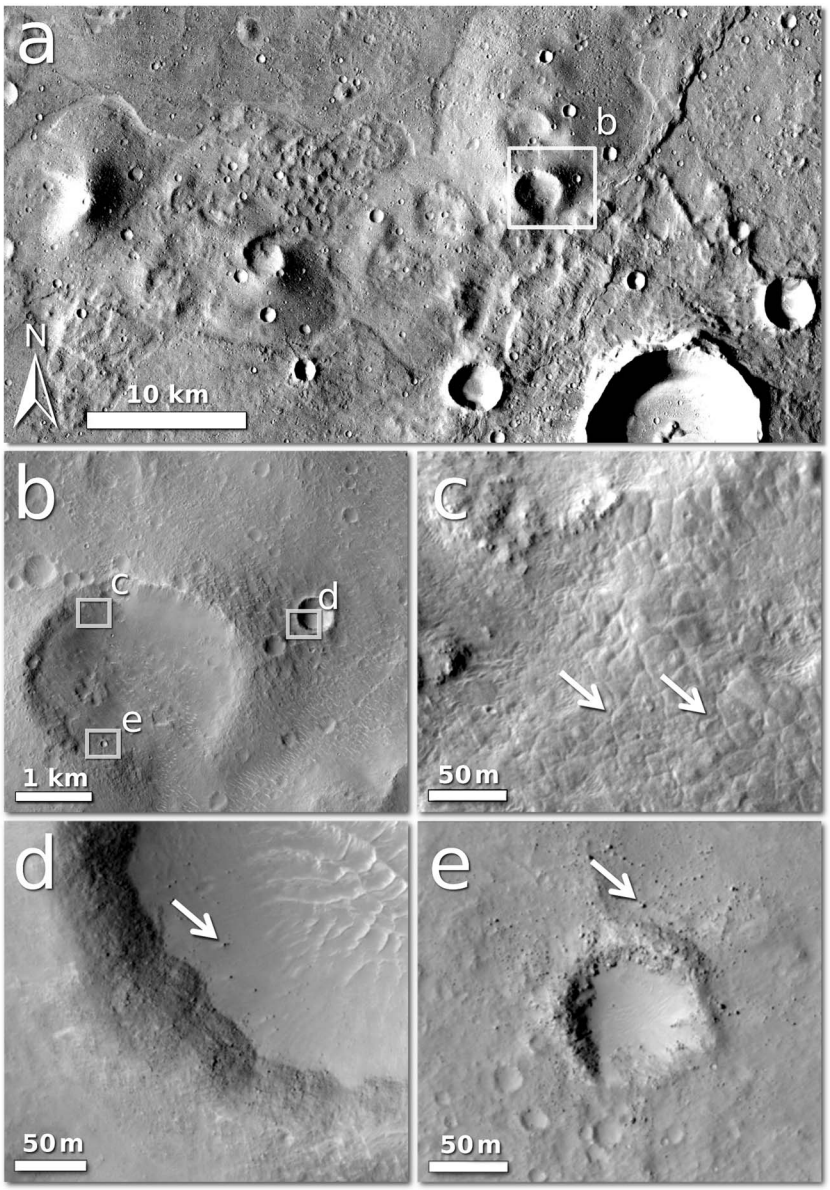

Figure 7. (a) Detail of one of the clusters of investigated NAC cones (16.59°N/104°E) (b) Pitted cone in the NAC field with well-developed central crater and steep inner flanks (detail of HiRISE image ESP_018776_1970; 16.65°N/104.15°E). (c) Detail of polygon-like pattern visible in some locations on the inner flank of the cone. (d and e) Large boulders associated with two impact craters, suggesting that the cone consists of consolidated material with some cohesive strength. The polygonal patterns may be related to a smooth mantling deposit, possibly suggesting a younger age than the main cone.

after the main period of fluvial activity on Mars [*Fassett and Head*, 2008].

5. Discussion

5.1. Evaluation of Arguments Against Igneous Volcanism

[27] In this section, we discuss the individual arguments used by *Skinner and Tanaka* [2007] to reject igneous volcanism. *Skinner and Tanaka* [2007] considered an igneous volcanic origin of the NAC unlikely because of (1) the large distance to known volcanic vents, (2) a lack of obvious structural control of dike-related eruptions, (3) the confinement to a specific latitude and elevation range, (4) the setting in a compressional tectonic regime, and (5) the pitted cones being part of a broader assemblage of landforms. We explore these arguments now to evaluate if they indeed disfavor an igneous origin. The distance to known volcanic vents may be smaller than previously thought, since localized spots of volcanism around the NAC region have by now being suggested by several subsequent studies [*Lanz and Saric*, 2009; *Lanz et al*., 2010; *de Pablo and Pacifici*, 2008; *de Pablo and Caprarelli*, 2010; *Ghent et al*., 2012]. A lack of obvious structural control of dike-related eruptions, first qualitatively assumed by *Skinner and Tanaka* [2007], can now be confirmed quantitatively by our test applying the two-point

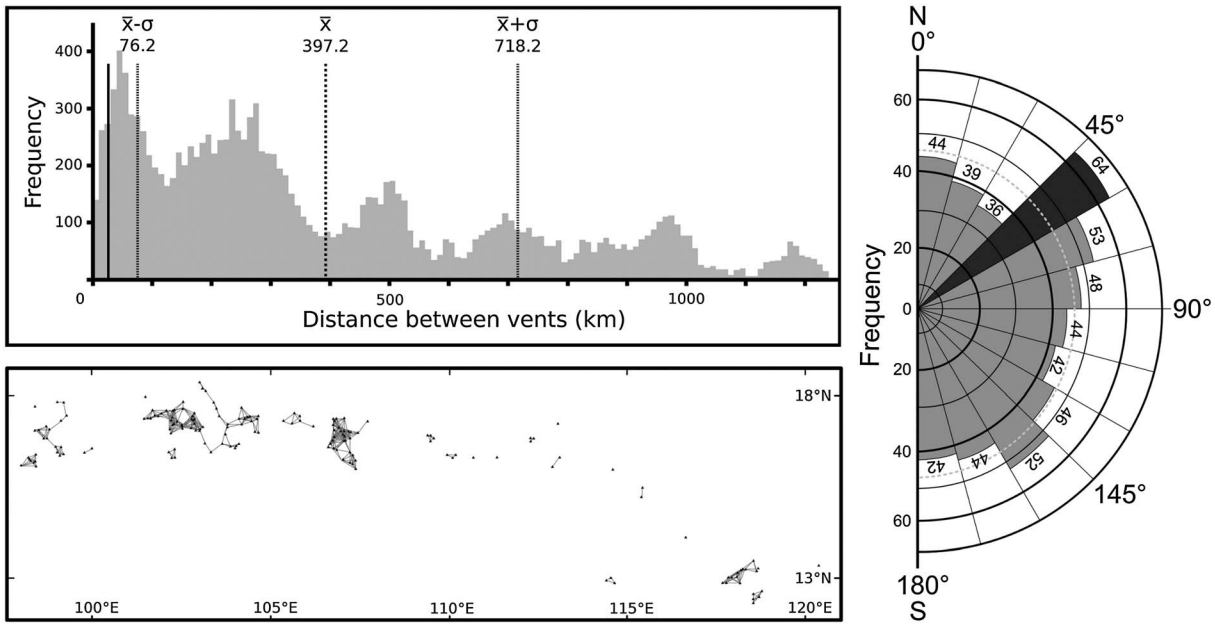

Figure 8. Results of the two-point azimuth technique. The upper left panel shows a frequency histogram of the lengths of lines connecting the NAC cones. Several peaks are visible due to the clustering of cones in the area of interest. The lower left panel shows the mapped distribution of lines with lengths ≤25.4 km, corresponding to the minimum significant distance (i.e., (x−1σ)/3) as defined by *Cebriá et al*. [2011]). Some NE-directed orientation of lineaments can be observed. The right part of the figure represents a rose diagram with 15° bin intervals, containing the numbers of lines per bin for lines ≤25.4 km long. The dotted line represents the arithmetic mean of frequency per bin (46.2, standard deviation 7.1), and the dark grey color marks the bin where frequency is higher than one standard deviation above the mean. This predominant orientation is in agreement with the lineaments observable in the mapped distribution.

azimuth method (Figure 8). At least one mound (Figure 6a) appears to be associated with a fissure that may represent an underlying dike, but this is not sufficient evidence for a general structural control. This lack of structural control, however, is not necessarily arguing in favor of mud volcanism, since mud volcanoes are themselves known to be controlled by tectonic structures [*Roberts et al*., 2011; *Bonini*, 2012]. The lack of structural control, therefore, does not seem to put constraints on either of the two possible formation hypotheses, igneous volcanism or mud volcanism. The confinement to a specific latitude and elevation range might be explained by the location along the dichotomy boundary (see below). The location of the cones in an area characterized by a compressional tectonic regime is not a strong argument against igneous volcanism, either. Although it has been widely held that volcanism can occur only in extensional tectonic regimes, favoring magma ascent along (sub)vertical fractures trending perpendicular to the least principal stress (σ_3), this axiom has been challenged. Based on an in situ investigation of El Reventador volcano in Ecuador, *Tibaldi* [2005] demonstrated that volcanism can also occur in compressional settings (the greatest principal stress σ_1 acting horizontally). He argued that magma can move upward in a compressional regime along vertical or subvertical planes which are oriented perpendicular to σ_2 (the direction of intermediate principal stress) and are related to reverse faulting associated to vertical σ_3. The assemblage of landforms is probably the strongest line of evidence provided by *Skinner and Tanaka* [2007] to support a formation of the NAC as mud volcanoes. However, at least one more of the landscape elements, the mounds, can also be explained by igneous volcanism (as it was done for mound-like structures elsewhere on Mars [cf. *Rampey et al*., 2007]). Morphologically analogous features are well known from terrestrial volcanic fields, whether basaltic or more silica rich in composition. These structures are a type of lava domes called coulees [*Fink and Anderson*, 2000]. They form by more viscous magma, effusively erupted onto the planetary surface and laterally spreading outward. Once the rate of the supplying magma decreases, the gravitational acceleration causes the outer parts to further flow outward, even without sufficient lava supplies. The flow thickens into a dome-like shape at the periphery, but a low amount of ascending magma is still able to build a small hill above the vent [*Hale et al*., 2007]. The result is a structure looking similar to the mounds in the Nephentes/Amenthes region (see Figure 6c for comparison). Similar structures, termed "festoon flows," were also observed on Venus [*Head et al*., 1992; *Moore et al*., 1992], where igneous volcanism is the only plausible explanation. We suggest therefore that the mounds can be interpreted as igneous volcanic mounds and are not unambiguous evidence for mud volcanism. This notion is further supported by the morphology of salt domes [e.g., see *Neish et al*., 2008, Figure 1c], which can be more or less identical and suggests that there is a type of landforms that are all produced by the surface extrusion of relatively high-viscous material, prohibiting unambiguous interpretation. The steep-sided depressions with irregular outlines in plan view named Amenthes Cavi, attributed to collapse following mud reservoir depletion at depth by *Skinner and Tanaka* [2007], are

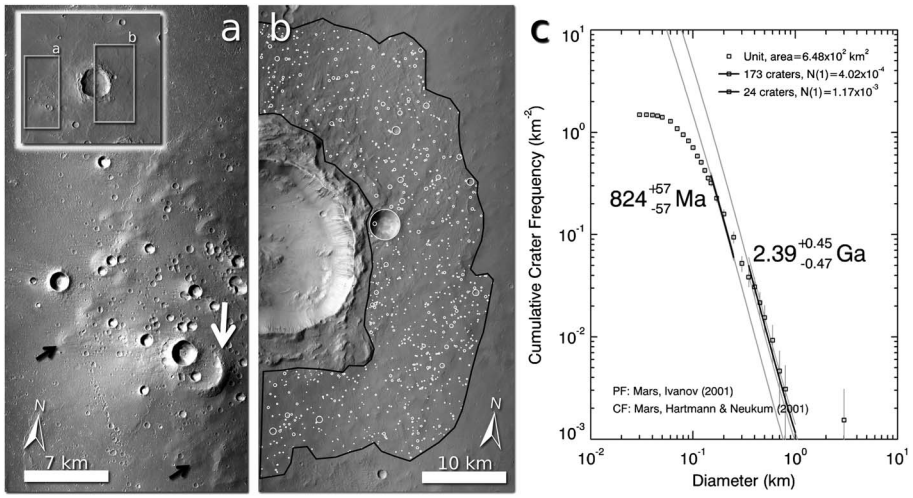

Figure 9. Absolute model age for ejecta of rampart crater embaying one of the NAC cones. See small inserted image for detail position. (a) Fluidized ejecta of this crater (marked by black arrows) are partly overlapping a small cluster of pitted cones (white arrow), suggesting that the crater is younger than these cones (detail of CTX image B19 016917 1976; centered at 17.84°N/99.09°E). Water ice had to be present in the subsurface at the time of rampart crater formation and hence was likely present at the time of cones formation, too. (b) Selected area for crater counting with marked craters (detail of CTX image P18_008056_1980; centered at 18.12°N/99.79°E). (c) Crater size-frequency distribution of ejecta. The cumulative crater frequency curve indicates an absolute model age of ~2.39 Ga.

not easily explained by the igneous volcanic scenario. They may be related to maars, and indeed maars such as Kilboune Hole and Hunt's Hole (New Mexico, USA) can display irregular shapes [cf. *Ollier*, 1967], but we are not able to further substantiate this hypothesis.

[28] The flow-like features emanating from the central vents of some cones might be explained by an insufficient source of subsurface water to fully fragment the ascending magma, so lava could leak out effusively from the central crater and produce a lava flow [*Basaltic Volcanism Study Project*, 1981; *Lorenz*, 1986]. However, the thick dust cover in the NAC region prevents identifying any surface flow structure of these hypothesized flows and distinguishing characteristic patterns of basaltic lava flows.

5.2. Morphometric Comparison With Terrestrial Analogues

[29] For comparison between different types of volcanoes, including mud volcanoes in Azerbaijan, we quantitatively measured parameters commonly used in the morphometric analyses of volcanic edifices (Table 2). A morphometric comparison of the cones in the study area with volcanic cones on Mars and Earth reveals that the NAC form a quite distinct group of edifices in a plot of W_{CR}/W_{CO} over W_{CO} (Figure 5). As compared to terrestrial pyroclastic edifices (cinder cones, tuff cones, maars), the NAC have larger basal diameters, but their W_{CR}/W_{CO} ratio is basically identical. As compared to terrestrial effusive edifices (low basaltic lava shields), the NAC have a similar range of basal diameters, but a distinctly higher W_{CR}/W_{CO} ratio. Moreover, low shields produced by effusive eruptions have larger basal diameters on Mars than on Earth, but very similar W_{CR}/W_{CO} ratios. The same observation seems to apply for cinder cones on Earth and Mars. Terrestrial mud volcanoes are different from the NAC both with respect to basal diameter and W_{CR}/W_{CO} ratio. It appears that for both explosive and effusive eruptions, edifices of the same type tend to be larger in diameter on Mars (i.e., shifted to the right in Figure 5). The W_{CR}/W_{CO} ratios, however, seem to be very similar, despite predictions that explosive eruptions may produce larger relative crater sizes on Mars, due to the lower gravity and atmospheric pressure [*Wilson and Head*, 1994]. Instead, the same W_{CR}/W_{CO} ratios on Mars and Earth may suggest that this ratio is perhaps independent of gravity and atmospheric pressure, as assumed by *Wood* [1979] and confirmed by measurements of the cinder cone field, Ulysses Colles, on Tharsis [*Brož and Hauber*, 2012]. In an attempt to explain this surprising fact, *Wood* [1979] assumed that the higher ejection velocities and the wider dispersal of pyroclasts equally affect crater rims and more distal deposits (W_{CO}).

[30] Importantly, the crater floors of many cones (13 out of 47 measured cones) in the NAC region have elevations at or below the surrounding plains (i.e., the preexisting ground level; see Table S.1 in the auxiliary material) (Figures 4b, 4c, and 4e), and the craters are surrounded by rims up to several dozen meters high. This does not seem to be consistent with the morphometry of terrestrial mud volcanoes. *Kholodov* [2002] summarized several different types of mud volcanoes on Earth, none of them having similar relief and size as observed with the NAC. For example, mud volcanoes forming a depressed syncline on the Kerch Peninsula in Ukraine have crater levels below the surrounding plains, similar to the NAC pitted cones, but they are lacking cones around vents, high rims surrounding these depressions, and they are surrounded by ring faults. On the other hand, mud volcanoes in Azerbaijan, offered as terrestrial analogues to the NAC by *Skinner and Tanaka* [2007], display conical shapes with heights of up to several hundred meters, again similar to the NAC, but without deeply excavated craters (for more details see *Kholodov* [2002, Figure 2], or

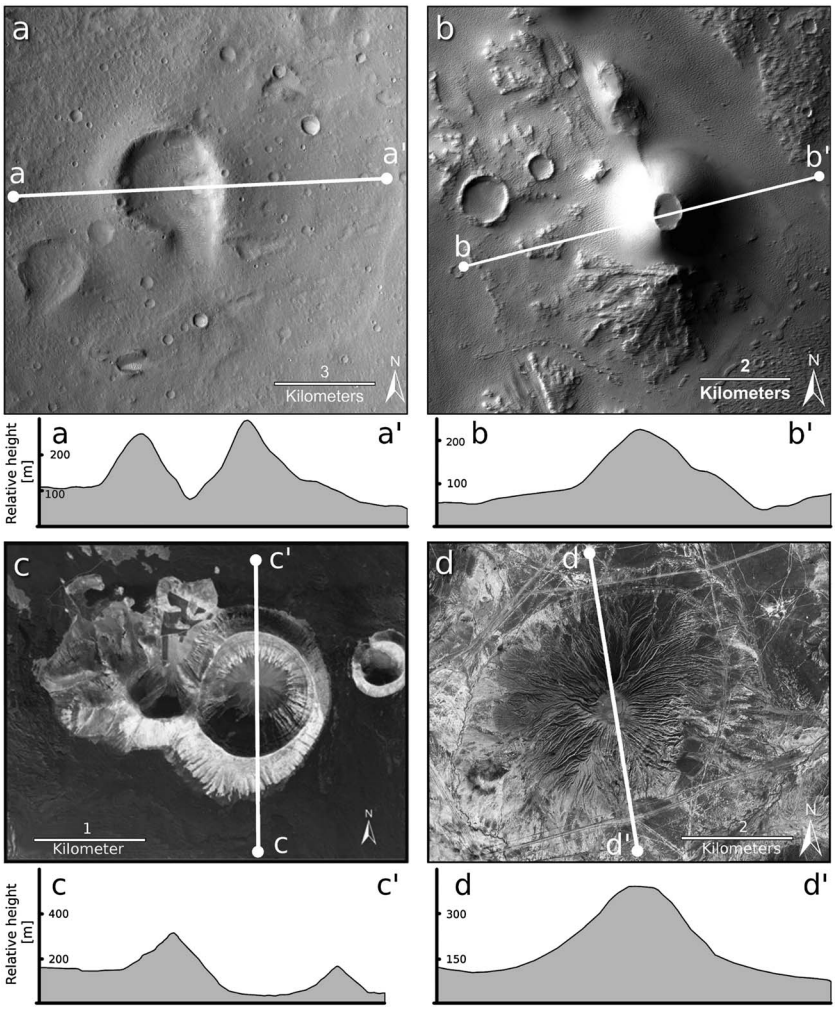

Figure 10. Different types of cones with topographic profiles. (a) Investigated pitted cone in the NAC field (detail of CTX image P17_007489_1967_ 16.32°N/102.32°E). (b) Steep-sided cone with associated flow-like structure in the Ulysses Colles cinder cone field in Tharsis, Mars (modified from *Brož and Hauber* [2012]; detail of CTX image P21_009409_1858, 5.69°N/237.05°E). (c) Tuff ring Caldera Blanca, Lanzarote (modified from *Kervyn et al*. [2012]; Figure 8d). (d) Mud volcano in Azerbaijan (image: Google Earth; 40.16°N/49.30°E) used by *Skinner and Tanaka* [2007] as terrestrial analogue for pitted cones in their study. Note the significant difference in cross-sectional shape between the pitted cone in the NAC field, displaying a crater with a depth equaling its height, and the Martian cinder cone. Terrestrial mud volcanoes typically lack a central deep and wide crater. On the other hand, morphological and topographical similarities are obvious between the NAC cone and the terrestrial tuff ring.

Table 1). Deep craters situated on top of cones are not a common feature of terrestrial mud volcanoes in Azerbaijan, and it appears that the morphologies of the NAC and the previously suggested analogues in Azerbaijan are inconsistent (see Figures 4 and 10).

[31] Another observation that appears to be possibly inconsistent with a mud volcano shape is a low cone with a double or nested crater (Figure 3c). The cone is situated in a cluster of pitted cones and some lobate flows. Based on relative stratigraphy, a similar age as the other cones in this cluster is inferred. This atypical cone is about 3.5 km wide and 60 m high, with clearly recognizable rims of the inner and outer crater in profiles. A double or nested crater morphology was already ascribed to Martian pseudocraters [*Noguchi and Kurita*, 2011] as a result of lava/water interaction; however, the described possible pseudocrater was smaller by an order of magnitude (about 130 m in diameter). On the other hand, similar structures with similar dimensions are known from Earth as a result of repeated phreatomagmatic activity formed by magma/water interaction. A characteristic example is the tuff ring Tagus Cove on Isabela Island (Galápagos archipelago, Ecuador), and another well-known feature with nested circular features in plan view is the maar, Split Butte, in the Snake River Plain, which consists of a tephra ring and the remnants of a lava lake [*Womer et al*., 1980]. It has to be noted, though, that nested craters have also been observed on terrestrial mud volcanoes [e.g., *Skinner and Mazzini*, 2009, Figures 6e and 6f].

[32] The HiRISE observation did not help to differentiate between an igneous versus a mud volcanic origin of the NAC cones, because a thick dust cover hides potentially diagnostic surface textures. In the case of boulders

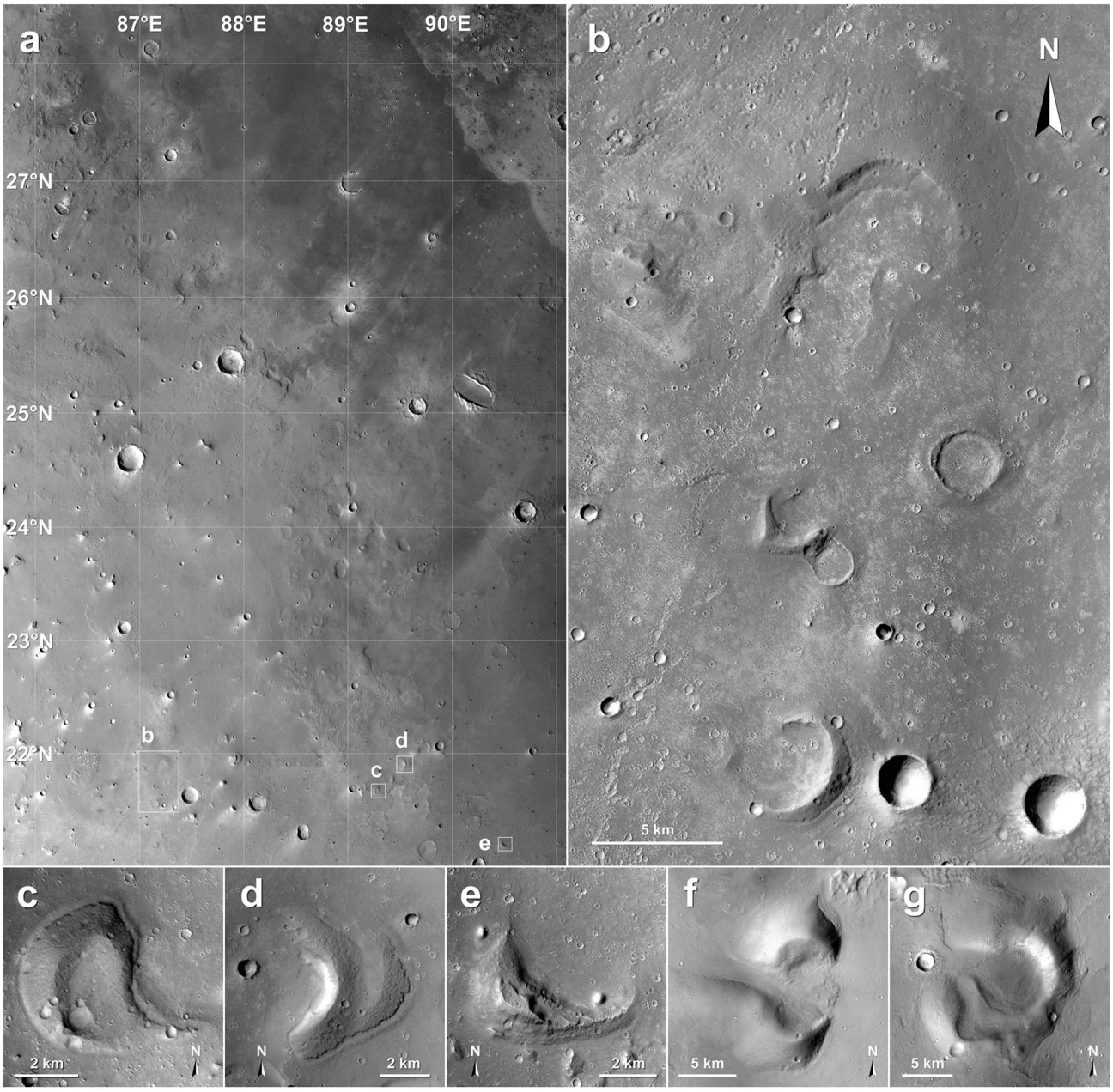

Figure 11. Pitted cones in the Arena Colles region. (a) Context image. Note the poor visibility of the cones, which are spread over the entire image. Letters b–e mark locations of Figures 11b–e. HRSC image mosaic (for location see Figure 1). (b) Group of cones with different sizes and rim appearance. While the rim of the cone in the middle right of the image is complete, the rims of all other cones are breached or only partly preserved (CTX image mosaic; see Figure 11a for location). (c) Breached cone (detail of CTX image G09_021572_2026; see Figure 11a for location). (d) Remnant of (breached?) cone (detail of CTX image B20_017392_2009; see Figure 11a for location). (e) Layered cone remnant (detail of CTX image B18_016825_2018; see Figure 11a for location). (f) Breached cone at 31.87°N/82.93°E (mosaic of CTX images G19_025594_2108 and P13_006158_2112). (g) Nested cones centered at 30.77°N/82.94°E (mosaic of CTX images G19_025594_2108 and P13_006158_2112). Note that Figures 11f and 11g are located outside the area shown in Figure 11a.

surrounding small impact craters, it is impossible to distinguish if they represent mud breccia or welded volcanic ash and/or volcanic bombs. Despite the fact that mud volcanoes on Earth are mainly formed by fine-grained material [*Manga and Bonini*, 2012], they may be able to carry larger clasts forming mud breccias [*Pondrelli et al*., 2011].

[33] We conclude that several morphometric aspects of the available data are more consistent with an igneous volcanic origin than with a mud volcano scenario, without ruling out the latter. In the next sections, we discuss the factors that would have been critical in an igneous volcanic model to explain the formation of the pitted cones and mounds.

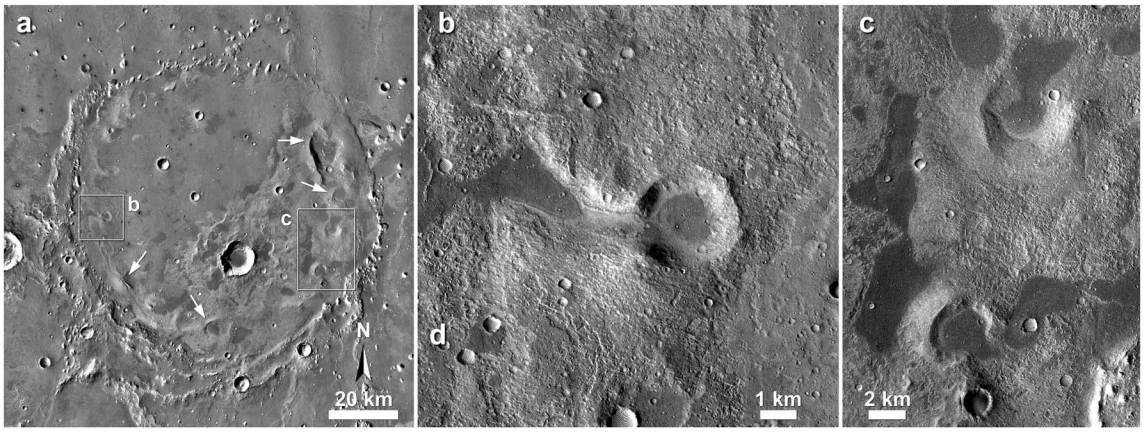

Figure 12. Cones of similar morphology in Xanthe Terra. (a) Lederberg crater (center 13.01°N, 314.08° E), a 90 km wide impact crater, is situated at the southern margin of Chryse Planitia at the dichotomy boundary. Along the inner crater rim, a series of small conical positive landforms with deep and wide craters can be observed (CTX image mosaic). (b and c) Examples of breached cones with morphology similar to the NAC cones. White arrows in Figure 12a point to other examples.

5.3. Other Regions With Morphologically Similar Landforms

[34] To find out whether the NAC represent a unique class of landforms on Mars, we searched for similar landforms in other areas near the dichotomy boundary. A field with cones of identical morphology was identified in the Arena Colles region north of Isidis Planitia (Figure 11). To our knowledge, it has never been mentioned in the literature before. The general context of this field seems to be comparable to that of the NAC, because it is also located on a topographical bench at the margin of the Utopia basin, and at the dichotomy boundary (Figure 1). Since this cone field is similar in morphology and in the geotectonic context, it could also be explained by the scenario of *Skinner and Tanaka* [2007], in particular by their annular space and basin setting and therefore does not provide additional arguments for one or the other formation hypothesis.

[35] Other similar cones were found in Xanthe Terra, at the southern margin of the ancient impact basin, Chryse (Figure 12). Xanthe Terra is part of the heavily cratered highlands dominated by Noachian terrain [*Rotto and Tanaka*, 1995]. It is surrounded by younger lava plains of Lunae Planum in the west, by Ophir Planum in the south, by chaotic terrain in the east, and by Chryse Planitia in the north. The area of interest is the ~90 km diameter impact crater, Lederberg, close to the dichotomy boundary and centered at 13.01°N/314.08°E. As the NAC and Arena Colles cone fields, Lederberg lies close to the dichotomy boundary [*Scott and Tanaka*, 1986] on the southern edge of the ancient impact basin, Chryse [*Schultz et al*., 1982]. In a regional context, this area displays evidence of past fluvial (outflow channels, river beds, river deltas, etc.), volcanic, and glacial activity [*Hauber et al*., 2009b, 2012; *Martínez-Alonso et al*., 2011]. A wide range of landforms caused by aqueous activity, including rampart craters, offers a plausible prerequisite for hydrovolcanic interactions due to the occurrence of subsurface water ice. Lederberg crater itself is filled with smooth material and hosts several cones with partly breached rims, which are aligned on the floor along its interior wall. These cones do not resemble impact craters, and their floors are at the same level with their surroundings. Based on the morphological similarity of these cones and the NAC cones, we suggest that the cones in Lederberg crater were also formed by a similar genesis, which we interpret to be possibly phreatomagmatic. Since the local tectonic environment of Lederberg crater is different from that of the NAC field, the formation of this type of cones may not require a unique geotectonic setting.

5.4. Hydrovolcanism

[36] Hydrovolcanism is a common phenomenon in all environments on Earth where water is mixing with magma [*Sheridan and Wohletz*, 1983]. The type of landforms which occurs depends on whether surges contain superheated steam media (in the case of tuff rings) or condensing steam media (tuff cones) [*Sheridan and Wohletz*, 1983]. Hydrovolcanic landforms are second in abundance on Earth to scoria cones only [*Vespermann and Schmincke*, 2000], and they represent the most common landforms created by explosive hydromagmatic volcanism [*Wohletz and Sheridan*, 1983]. Phreatomagmatic eruptions can occur with magma of various compositions, both basaltic and more evolved [*Wohletz and McQueen*, 1984a, 1984b]. All prerequisites for phreatomagmatic eruptions are encountered on Mars: (basaltic) volcanism and crustal water/ice, both widely spread around the planet in space and time [*Grott et al*., 2013; *Lasue et al*., 2013]. Hence, we may reasonably expect that hydrovolcanism operated on Mars. However, direct observations of phreatomagmatic landforms on Mars (especially tuff rings, tuff cones, and maars) are sparse and published reports are not very detailed [*Wilson and Mouginis-Mark*, 2003a, 2003b; *Wilson and Head*, 2004, *Keszthelyi et al*., 2010].

[37] Terrestrial tuff rings and tuff cones are generally small (less than 5 km in diameter) monogenetic volcanoes composed of tuff that results from hydrovolcanic (hydromagmatic) explosions. They display well-developed, relatively large craters (large W_{CR}/W_{CO} ratio), and the crater

floors of tuff rings and tuff cones extend down to and even below the level of the preexisting surface level, respectively [*Wohletz and Sheridan*, 1983; *Leach*, 2011]. Tuff rings have normally low topographic profiles and gentle external slopes ranging from 2° to 15° [*Sheridan and Wohletz*, 1983], and they are underlain by shallow diatremes [*Lorenz*, 1986; *White and Ross*, 2011]. On the other hand, tuff cones have high profiles with steep outer slopes [*Wohletz and Sheridan*, 1983] ranging from 25° to 30° [*Sheridan and Wohletz*, 1983] without underlying diatremes [*White and Ross*, 2011]. Both classes of tuff edifices have generally asymmetric rims caused by wind moving ash in downwind direction [*Farrand et al*., 2005], or by a change of vent location and multiple vents with different production rates [*Sheridan and Wohletz*, 1983]. Maars are volcanic depressions that have typical widths of several hundred meters. They are underlain by deep diatremes and lie below the level of the surrounding unit [*Lorenz*, 1986].

[38] In general, the observed morphology, shape, and size of the pitted cones in our study area are similar to those of terrestrial tuff cones or rings, except for a larger absolute basal diameter. We note, however, that cone morphometry alone is not a reliable indicator for eruptive conditions. The results can be affected by difficulties in determining the correct basal perimeter of the edifice [*Grosse et al*., 2012], by slope angle variations within a single cone [*Kereszturi et al*., 2012], by the effects of cone burial by later deposits [*Favalli et al*., 2009], and by other factors such as the applied methodology, the local setting, time-dependent eruption conditions, and material properties [*Kervyn et al*., 2012]. Although the clear distinction of the NAC cones from other edifices (Figure 5) appears to be a robust result, we interpret that these features may not all be tuff cones or tuff rings. Instead, it is typical on Earth that volcanic fields are formed by several types of monogenetic volcanoes overlapping each other. *Wohletz and Sheridan* [1983] noted that a dry environment would contain cinder cones, whereas tuff rings may occur in places with abundant ground water source, and tuff cone formation would be favored by a shallow body of standing water. Moreover, even an individual cone can change its eruption style from an initially phreatomagmatic stage to a final Strombolian activity [*Clarke et al*., 2009]. Because of this variability, it is reasonable to expect that some of investigated NAC might represent cinder cones formed by magma degassing, and therefore it would be too simplistic to ascribe all NAC edifices to a single eruption type. More likely, we interpret that the history of NAC formation was diverse and several volcanic processes took place (degassing and water/magma interaction) and overlap each other. In fact, the mounds would represent a more effusive type of eruption if our interpretation is correct. Nevertheless, we suggest that the dominant volcanic process forming the NAC field was hydrovolcanism, producing cones by phreatomagmatic eruptions.

5.5. Origin of Magmatism

[39] We now explore if there are plausible geodynamic scenarios that would explain the occurrence of igneous volcanism in the study area. The cones occur within an elongated zone of ~1500 km length and 200 km width that is oriented roughly parallel to the highland-lowland scarp. Together with other hypothesized volcanic centers [*Lanz et al*., 2010; *Ghent et al*., 2012; *de Pablo and Pacifici*, 2008; *de Pablo and Caprarelli*, 2010], this zone would be part of a wide zone of magmatic activity that spans from the Elysium bulge in the east to Isidis Planitia to the west (Figure 1). It has to be noted, however, that alternative interpretations exist for several of these localized volcanic centers (e.g., for the pitted cones in Isidis Planitia), so without further confirmation they only provide weak support for an igneous scenario.

[40] Modeling by *McGovern and Litherland* [2011] shows that loading stresses due to the magmatic infilling of large (compared to the planetary radius) impact basins can induce at basin margins a favorable combination of extensional membrane stresses and upward-increasing extensional flexural stresses (positive "tectonic stress gradient" [*Rubin*, 1995]). Such conditions can create favorable environments for magma ascent in annular zones around basins that can drive the ascent of magma in dikes directly from mantle melt zones to the surface [*McGovern et al*., 2011]. The annular ring basins inferred by *Skinner and Tanaka* [2007] would be consistent with such a scenario as well as with the mud volcano hypothesis. Indeed, the studied cones are located within the Utopia-circumferential zones of maximum likelihood of magma ascent [*McGovern et al*., 2011], and the densest population of cones (in the western part of the study area) is situated near the overlap of this zone and the corresponding zone concentric to the Isidis basin. The location of a newly detected cone field in the Arena Colles region (see below) also fits to the same zone circumferential to Utopia (Figure 1). It appears possible therefore that igneous volcanism was focused in the study area by basin-related effects as described by *McGovern and Litherland* [2011].

[41] Igneous volcanism may also be explained by the location of the NAC along the dichotomy boundary. The bench or boundary plain on which the pitted cones are located lies along a zone of extension that parallels the topographic scarp of the dichotomy boundary between eastern Arabia and Cimmeria Terrae [*Watters*, 2003] (Figure 1), which also marks the transition of thicker crust in the south to thinner crust in the north [*Zuber et al*., 2000]. Lower-crustal flow from thick crust in the south toward thinner crust in the north may be able to induce extension (favorable for magma ascent) just north of the highland-lowland scarp [*Nimmo*, 2005]. It has also been speculated [cf. *Zuber et al*., 2000] that thick accumulations of volcanic material could explain the positive Bouguer anomalies along this part of the dichotomy boundary [*Neumann et al*., 2004]. Hence, past volcanism seems to be plausible at the study site, and indeed the relatively high dielectric constant of the substrate at the study area [*Mouginot et al*., 2012] is consistent with this possibility.

[42] If our interpretation of explosive (hydro)volcanism in the NAC field and in Arena Colles is true, some implications for the global view on Martian magmatism may be inferred. The style of volcanism on Mars appears to be diverse and includes hydromagmatism, as we may expect on a volcanically active planet with widespread evidence for water and ice in the subsurface.

[43] The study area containing the NAC field is located west of the light-toned layered Medusae Fossae Formation (MFF), which consists of a material that is either ice rich or, if dry, has a low density [*Watters et al*., 2007] and would be consistent with a volcanic airfall deposit [e.g., *Bradley et al*., 2002]. It has been suggested that the large volcano, Apollinaris Patera, might be the source of the dispersed

volcanic clasts that build the MFF [*Kerber et al*., 2012], but the volume of the MFF seems large compared to Apollinaris Patera. The dispersal of pyroclasts from the NAC field in an ESE direction (assuming a speculative dominant WNW wind direction; Figure 1) may have contributed to the deposition of the MFF and would lessen the volume problem.

6. Conclusions

[44] 1. Pitted cones along the southern margin of Utopia Planitia share morphological similarities to terrestrial tuff cones and tuff rings. A hydrovolcanic origin of these cones is consistent with the observed morphology and the regional geologic setting. Mounds associated with the cones resemble terrestrial lava domes (coulees). Together, we interpreted these landforms as a volcanic field.

[45] 2. Another field with identical landforms was newly detected north of Isidis Planitia in the Arena Colles region, also along the margin of Utopia Planitia. Several cones in an impact crater Lederberg in Xanthe Terra share the same morphological characteristics. These new observations of this type of pitted cones suggest that their formation may not require unique tectonic or environmental conditions.

[46] 3. While the consistent mud volcano scenario of *Skinner and Tanaka* [2007] cannot be ruled out, several points used previously against an igneous volcanic origin of these landforms have been reevaluated. The geotectonic setting and the growing evidence for additional volcanic centers in the wider region would be consistent with igneous volcanism. The general lack of obvious structural control is not a conclusive argument, as structural control would be expected for both igneous and mud volcanism. The spatial association with Amenthes Cavi, as postulated by *Skinner and Tanaka* [2007], however, is not explained by an igneous volcanic scenario.

[47] 4. If our interpretations are correct, they would add to the morphologic diversity of Martian volcanic surface features. To our knowledge, however, the total number of similar landforms on Mars is low. Given that subsurface water was likely widespread in Martian history, this prompts the question as to why hydrovolcanic landforms are not observed more frequently. One possible answer is that phreatomagmatic eruptions were indeed more frequent in the past, but much of their traces have now been eroded, and the fields reported here are among the latest to be formed.

[48] 5. If mud volcanism is the process of NAC formation, then the process varies from terrestrial mud volcanism in producing morphologically varied forms and warrants further study. More morphometric work is needed for terrestrial mud volcanoes, including mud volcanoes in areas other than Azerbaijan, so that we can more accurately assess the comparison with morphologically similar landforms on Mars.

[49] **Acknowledgments.** We would like to thank Václav Kuna for his help with the two-point azimuth technique and Rina Noguchi for her useful hints about phreatomagmatic landforms. Jim Skinner kindly provided helpful comments on some aspects of the manuscript. Three detailed and constructive reviews by David Williams, Peter Mouginis-Mark, and Jim Skinner greatly improved the manuscript. We appreciate the efforts of the instrument teams (MOLA, HRSC, CTX, HiRISE) that acquired and archived most of the data used in our investigation. This study was partly supported by the Helmholtz Association through the research alliance "Planetary Evolution and Life," and by grant 4400-243-253452 of the program of the Charles University Science Foundation GAUK.

References

Baker, V. R. (2001), Water and the martian landscape, *Nature*, *412*, 228–236, doi:10.1038/35084172.

Basaltic Volcanism Study Project (1981), *Basaltic Volcanism on the Terrestrial Planets*, 1286 pp., Pergamon Press, Inc., New York.

Bleacher, J. E., R. Greeley, D. A. Williams, S. R. Cave, and G. Neukum (2007), Trends in effusive style at the Tharsis Montes, Mars, and implications for the development of the Tharsis province, *J. Geophys. Res.*, *112*, E09005, doi:10.1029/2006JE002873.

Bleacher, J. E., L. S. Glaze, R. Greeley, E. Hauber, S. M. Baloga, S. E. H. Sakimoto, D. A. Williams, and T. D. Glotch (2009), Spatial and alignment analyses for a field of small volcanic vents south of Pavonis Mons and implications for the Tharsis province, Mars, *J. Volcanol. Geotherm. Res.*, *185*, 96–102, doi:10.1016/j.jvolgeores.2009.04.008.

Bonini, M. (2012), Mud volcanoes: Indicators of stress orientation and tectonic controls, *Earth Sci. Rev.*, *115*, 121–152, doi:10.1016/j.earscirev.2012.09.002.

Bradley, B. A., S. E. H. Sakimoto, H. Frey, and J. R. Zimbelman (2002), Medusae Fossae Formation: New perspectives from Mars Global Surveyor, *J. Geophys. Res.*, *107*(E8), 5058, doi:10.1029/2001JE001537.

Brož, P., and E. Hauber (2012), An unique volcanic field in Tharsis, Mars: Pyroclastic cones as evidence for explosive eruptions, *Icarus*, *218*(1), 88–99, doi:10.1016/j.icarus.2011.11.030.

Buisson, C., and O. Merle (2002), Experiments on internal strain in lava dome cross sections, *Bull. Volcanol.*, *64*, 363–371, doi:10.1007/s00445-002-0213-6.

Burr, D. M., B. C. Bruno, P. D. Lanagan, L. S. Glaze, W. L. Jaeger, R. J. Soare, J.-M. Wan Bun Tseung, J. A. Skinner, and S. M. Baloga (2009), Mesoscale raised rim depressions (MRRDs) on Earth: A review of the characteristics, processes, and spatial distributions of analogs for Mars, *Planet. Space Sci.*, *57*, 579–596, doi:10.1016/j.pss.2008.11.011.

Byrne, S., et al. (2009), Distribution of Mid-Latitude Ground Ice on Mars from New Impact Craters, *Science*, *325*, 1674–1676, doi:10.1126/science.1175307.

Carr, M. H., and J. W. Head (2010), Geologic history of Mars, *Earth Planet. Sci. Lett.*, *294*(3–4), 185–203, doi:10.1016/j.epsl.2009.06.042.

Carr, M. H., R. Greeley, K. R. Blasius, J. E. Guest, and J. B. Murray (1977), Some martian volcanic features as viewed from the Viking Orbiters, *J. Geophys. Res.*, *82*, 3985–4015, doi:10.1029/JS082i028p03985.

Carruthers, M. W., and G. W. McGill (1998), Evidence for igneous activity and implications for the origin of a fretted channel in southern Ismenius Lacus, Mars, *J. Geophys. Res.*, *103*, 31,433–31,443, doi:10.1029/98JE02494.

Cashman, K. V., B. Sturtevant, P. Papale, and O. Navon (1999), Magmatic Fragmentation, in *Encyclopedia of volcanoes*, edited by H. Sigurdsson, pp. 421–430, Academic Press, San Diego, California.

Cebriá, J.-M., C. Martín-Escorza, J. López-Ruiz, D. J. Morán-Zenteno, and B. M. Martiny (2011), Numerical recognition of alignments in monogenetic volcanic areas: Examples from the Michoacán-Guanajuato Volcanic Field in Mexico and Calatrava in Spain, *J. Volcanol. Geoth. Res.*, *201*, 73–82, doi:10.1016/j.jvolgeores.2010.07.016.

Clark, P. J., and F. C. Evans (1954), Distance to nearest neighbour as a measure of spatial relationships in populations, *Ecology*, *35*, 445–453, doi:10.2307/1931034.

Clarke, H., V. R. Troll, and J. C. Carracedo (2009), Phreatomagmatic to Strombolian eruptive activity of basaltic cinder cones: Montaña Los Erales, Tenerife, Canary Islands, *J. Volcanol. Geotherm. Res.*, *180*, 225–245, doi:10.1016/j.jvolgeores.2008.11.014.

Connor, C. B. (1990), Cinder cone clustering in the TranMexican Volcanic Belt: Implications for structural and petrologic models, *J. Geophys. Res.*, *95*, 19,395–19,405.

Connor, C. B., and F. M. Conway (2000), Basaltic volcanic Fields, in *Encyclopedia of volcanoes*, edited by H. Sigurdsson, pp. 313–343, Academic Press, San Diego, California.

Crater Analysis Techniques Working Group (1979), Standard techniques for presentation and analysis of crater size–frequency data, *Icarus*, *37*, 467–474, doi:10.1016/0019-1035(79)90009-5.

Ennis, M. E., M. E. Schmidt, T. McCoy, W. Farrand, and N. Cabrol (2007), Hydorvolcano on Mars? A comparison of Home Plate, Gusev Crater and Zuni Salt Lake Maar, New Mexico, Lunar Planet. Sci. 38, abstract 1966.

Erkeling, G., H. Hiesinger, D. Reiss, F. J. Hielscher, and M. A. Ivanov (2011), The stratigraphy of the Amenthes region, Mars: Time limits for the formation of fluvial, volcanic and tectonic landforms, *Icarus*, *215*, 128–152, doi:10.1016/j.icarus.2011.06.041.

Erkeling, G., D. Reiss, H. Hiesinger, J. Carter, M. A. Ivanov, E. Hauber, and R. Jaumann (2012), Valleys, paleolakes and possible shorelines at the Libya Montes/Isidis boundary: Implications for the hydrologic evolution of Mars, *Icarus*, *219*(1), 393–413, doi:10.1016/j.icarus.2012.03.012.

Farr, T. G., et al. (2007), The Shuttle Radar Topography Mission, *Rev. Geophys.*, *45*, RG2004, doi:10.1029/2005RG000183.

Farrand, W. H., L. R. Gaddis, and L. Keszthelyi (2005), Pitted cones and domes on Mars: Observations in Acidalia Planitia and Cydonia Mensae using MOC, THEMIS, and TES data, *J. Geophys. Res.*, *110*, E05013, doi:10.1029/2004JE002297.E05005.

Fassett, C. I., and J. W. Head (2008), The timing of martian valley network activity: constraints from buffered crater counting, *Icarus*, *195*, 61–89, doi:10.1016/j.icarus.2007.12.009.

Favalli, M., D. Karátson, F. Mazzarini, M. T. Pareschi, and E. Boschi (2009), Morphometry of scoria cones located on a volcano flank: A case study from Mt. Etna (Italy), based on high-resolution LiDAR data, *J. Volcanol. Geotherm. Res.*, *186*(3-4), 320–330, doi:10.1016/j.jvolgeores.2009.07.011.

Feldman, W. C., et al. (2004), Global distribution of near-surface hydrogen on Mars, *J. Geophys. Res.*, *109*, E09006, doi:10.1029/2003JE002160.

Fink, J. H., and S. W. Anderson (2000), Lava domes and coulees, in *Encyclopedia of volcanoes*, edited by H. Sigurdsson, pp. 307–319, Academic Press, San Diego, California.

Ghent, R. R., S. W. Anderson, and T. M. Pithawala (2012), The formation of small cones in Isidis Planitia, Mars through mobilization of pyroclastic surge deposits, *Icarus*, *217*(1), 169–183, doi:10.1016/j.icarus.2011.10.018.

Gilichinsky, M., D. Melnikov, I. Melekestsev, N. Zaretskaya, and M. Inbar (2010), Morphometric measurements of cinder cones from digital elevation models of Tolbachik volcanic field, central Kamchatka, *Can. J. Remote Sens.*, *36*, 287–300.

Google Inc. (2011), Google Earth (Version 6.1.0.5001) [Software], Available from http://www.google.com/earth/

Greeley, R. (1973), Mariner 9 photographs of small volcanic structures on Mars, *Geology*, *1*, 175–180, doi:10.1130/0091-7613(1973)1<175:MPOSVS>2.0.CO;2.

Greeley, R., and P. D. Spudis (1981), Volcanism on Mars, *Rev. Geophys. Space Phys.*, *19*, 13–41.

Grosse, P., B. van Wyk de Vries, P. A. Euillades, M. Kervyn, and I. Petrinovic (2012), Systematic morphometric characterization of volcanic edifices using digital elevation models, *Geomorphology*, *136*, 114–131, doi:10.1016/j.geomorph.2011.06.001.

Grott, M., et al. (2013), Long-term evolution of the Martian crust-mantle system, *Space Sci. Rev.*, *174*, 49–111, doi:10.1007/s11214-012-9948-3.

Guth, P. L. (2006), Geomorphometry from SRTM: Comparison to NED, PE&RS, *72*, 269–277.

Gwinner, K., F. Scholten, F. Preusker, S. Elgner, T. Roatsch, M. Spiegel, R. Schmidt, J. Oberst, R. Jaumann, and C. Heipke (2009), Topography of Mars from global mapping by HRSC high-resolution digital terrain 2 models and orthoimages: Characteristics and performance, *Earth Planet. Sci. Lett.*, *294*, 506–519, doi:10.1016/j.epsl.2009.11.007.

Hale, H. J., L. Bourgouin, and H.-B. Mühlhaus (2007), Using the level-set method to model endogenous lava dome growth, *J. Geophys. Res.*, *112*, B03213, doi:10.1029/2006JB004445.

Hamilton, C. W., S. A. Fagents, and T. Thordarson (2011), Lava-ground ice interactions in Elysium Planitia, Mars: Geomorphological and geospatial analysis of the Tartarus Colles cone groups, *J. Geophys. Res.*, *116*, E03004, doi:10.1029/2010JE003657.

Hartmann, W. K., and G. Neukum (2001), Cratering chronology and the evolution of Mars, *Space Sci. Rev.*, *96*(1/4), 165–194.

Hasenaka, T., and I. S. E. Carmichael (1985), A compilation of location, size, and geomorphological parameters of volcanoes of the Michoacán-Guanajuato volcanic field, Central Mexico, *Geofis.Int.*, *24-4*, 577–607.

Hauber, E., J. Bleacher, K. Gwinner, D. Williams, and R. Greeley (2009a), The topography and morphology of low shields and associated landforms of plains volcanism in the Tharsis region of Mars, *J. Volcanol. Geotherm. Res.*, *185*, 69–95, doi:10.1016/j.jvolgeores.2009.04.015.

Hauber, E., K. Gwinner, M. Kleinhans, D. Reiss, G. Di Achille, G.-G. Ori, F. Scholten, L. Marinangeli, R. Jaumann, and G. Neukum (2009b), Sedimentary deposits in Xanthe Terra: Implications for the ancient climate on Mars, *Planet. Space Sci.*, *57*(8-9), 944–957, doi:10.1016/j.pss.2008.06.009.

Hauber, E., P. Brož, F. Jagert, P. Jodłowski, and T. Platz (2011), Very recent and widespread basaltic volcanism on Mars, *Geophys. Res. Lett. 28*, L10201, doi:10.1029/2011GL047310.

Hauber, E., T. Platz, M. Kleinhans, L. Le Deit, P. Carbonneau, T. De Haas, W. Marra, and D. Reiss (2012), Old or Not So Old: That is the Question for Deltas and Fans in Xanthe Terra, Mars, Third Conference on Early Mars, abstract #7078.

Head, J. W., L. S. Crumpler, J. C. Aubele, J. E. Guest, and R. S. Saunders (1992), Venus volcanism - Classification of volcanic features and structures, associations, and global distribution from Magellan data, *J. Geophys. Res.*, *97*, 13,153–13,197, doi:10.1029/92JE01273.

Head, J. W., M. A. Kreslavsky, and S. Pratt (2002), Northern lowlands of Mars: Evidence for widespread volcanic flooding and tectonic deformation in the Hesperian Period, *J. Geophys. Res.*, *107*(E1), 5003, doi:10.1029/2000JE001445.

Inbar, M., and C. Risso (2001), A morphological and morphometric analysis of a high density cinder cone volcanic field – Payun Matru, south-central Andes, Argentina, *Z. Geomorphol.*, *45*, 321–343.

Ivanov, B. A. (2001), Mars/Moon Cratering Rate Ratio Estimates, *Space Sci. Rev.*, *96*(1/4), 87–104, doi:10.1023/A:1011941121102.

Ivanov, M. A., H. Hiesinger, G. Erkeling, F. J. Hielscher, and D. Reiss (2012), Major episodes of geologic history of Isidis Planitia on Mars, *Icarus*, *218*(1), 24–46, doi:10.1016/j.icarus.2011.11.029.

Jarvis, A., H. I. Reuter, A. Nelson, and E. Guevara (2008), Hole-filled SRTM for the globe Version 4, available from the CGIAR-CSI SRTM 90m Database (http://www.cgiar-csi.org/data/elevation/item/45-srtm-90m-digital-elevation-database-v41).

Jaumann, R., et al. (2007), The high-resolution stereo camera (HRSC) experiment on Mars Express: Instrument aspects and experiment conduct from interplanetary cruise through the nominal mission, *Planet. Space Sci.*, *55*, 928–952.

Kerber, L., J. W. Head, J.-B. Madeleine, F. Forget, and L. Wilson (2012), The dispersal of pyroclasts from ancient explosive volcanoes on Mars: Implications for the friable layered deposits, *Icarus*, *219*, 358–381, doi:10.1016/j.icarus.2012.03.016.

Kereszturi, G., G. Jordan, K. Németh, and J. F. Dóniz-Páez (2012), Syneruptive morphometric variability of monogenetic scoria cones, *Bull. Volcanol.*, *74*, 2171–2185, doi:10.1007/s00445-012-0658-1.

Kervyn, M., F. Kervyn, R. Goossens, S. K. Rowland, and G. G. J. Ernst (2007), Mapping volcanic terrain using high-resolution and 3D satellite remote sensing, in *Mapping Hazardous Terrain using Remote Sensing*, Special Publications 283, edited by R. M. Teeuw, pp. 5–30, Geological Society, London, doi:10.1144/SP283.2.

Kervyn, M., G. G. J. Ernst, P. Goossens, and P. Jacobs (2008), Mapping volcano topography with remote sensing: ASTER vs. SRTM, *Int. J. Remote Sens.*, *29*(22), 6515–6538, doi:10.1080/01431160802167949.

Kervyn, M., G. G. J. Ernst, J.-C. Carracedo, and P. Jacobs (2012), Geomorphometric variability of "monogenetic" volcanic cones: Evidence from Mauna Kea, Lanzarote and experimental cones, *Geomorphology*, doi:10.1016/j.geomorph.2011.04.009.

Keszthelyi, L., W. Jaeger, A. McEwen, L. Tornabene, R. A. Beyer, C. Dundas, and M. Milazzo (2008), High Resolution Imaging Science Experiment (HiRISE) images of volcanic terrains from the first 6 months of the Mars Reconnaissance Orbiter primary science phase, *J. Geophys. Res.*, *113*, E04005, doi:10.1029/2007JE002968.

Keszthelyi, L. P., W. L. Jaeger, C. M. Dundas, S. Martínez-Alonso, A. S. McEwen, and M. P. Milazzo (2010), Hydrovolcanic features on Mars: Preliminary observations from the first Mars year of HiRISE imaging, *Icarus*, *205*, 211–229, doi:10.1016/j.icarus.2009.08.020.

Kholodov, V. N. (2002), Mud volcanoes: Distribution regularities and genesis (Communication 2. geological–geochemical peculiarities and formation model), *Lithol. Miner. Resour.*, *37*, 293–310, doi:10.1023/A:1019955921606.

Kienzle, S. (2004), The effect of DEM raster resolution on first order, second order and compound terrain derivatives, *Trans. GIS*, *8*, 83–111.

Kneissl, T., S. van Gasselt, and G. Neukum (2011), Map-projection-independent crater size-frequency determination in GIS environments – new software tool for ArcGIS, *Planet. Space Sci.*, *59*, 1243–1254, doi:10.1016/j.pss.2010.03.015.

Konrad, J.-M., and R. Ayad (1987), An idealized framework for the analysis of cohesive soils undergoing desiccation, *Canad. Geotech. J.*, *34*(4), 477–488, doi:10.1139/t97-015.

Lanz, J. K., and M. B. Saric (2009), Cone fields in SW Elysium Planitia: Hydrothermal venting on Mars?, *J. Geophys. Res.*, *114*, E02008, doi:10.1029/2008JE003209.

Lanz, J. K., R. Wagner, U. Wolf, J. Kröchert, and G. Neukum (2010), Rift zone volcanism and associated cinder cone field in Utopia Planitia, Mars, *J. Geophys. Res.*, *115*, E12019, doi:10.1029/2010JE003578.

Lasue, J., N. Mangold, E. Hauber, S. Clifford, W. Feldman, O. Gasnault, C. Grima, S. Maurice, and O. Mousis (2013), Quantitative Assessments of the Martian Hydrosphere, *Space Sci. Rev.*, *174*, 155–212, doi:10.1007/s11214-012-9946-5.

Leach, J. H. J. (2011), The Tuff Rings of South East Australia and the Surficial Deposits of Mars: A Cautionary Tale, 42nd Lunar and Planetary Science Conference, abstract#1020.

Lorenz, V. (1986), On the growth of maars and diatremes and its relevance to the formation of tuff rings, *Bull. Volcanol.*, *48*, 265–274, doi:10.1007/BF01081755.

Lorenz, V. (1987), Phreatomagmatism and its relevance, *Chem. Geol.*, *62*, 149–156, doi:10.1016/0009-2541(87)90066-0.

Lutz, T. M. (1986), An analysis of the orientations of large-scale crustal structures: A statistical approach based on areal distributions of pointlike features, *J. Geophys. Res.*, *91*, 421–434, doi:10.1029/JB091iB01p00421.

Lutz, T. M., and J. T. Gutmann (1995), An improved method for determining and characterizing alignments of point-like features and its implications for the Pinacate volcanic field, Sonoran, Mexico, *J. Geophys. Res.*, *100*, 17,659–17,670, doi:10.1029/95JB01058.

Malin, M. C. (1977), Comparison of volcanic features of Elysium (Mars) and Tibesti (Earth), *Geol. Soc. Am. Bull.*, *88*, 908–919.

Malin, M. C., et al. (2007), Context camera investigation on board the Mars Reconnaissance Orbiter, *J. Geophys. Res.*, *112*, E05S04, doi:10.1029/2006JE002808.

Manga, M., and M. Bonini (2012), Large historical eruptions at subaerial mud volcanoes, Italy, *Nat. Hazards Earth Syst. Sci.*, *12*, 3377–3386, doi:10.5194/nhess-12-3377-2012.

Martínez-Alonso, S., M. T. Mellon, M. E. Banks, L. P. Keszthelyi, A. S. McEwen, and The HiRISE Team (2011), Evidence of volcanic and glacial activity in Chryse and Acidalia Planitiae, Mars, *Icarus*, *212*, 597–621, doi:10.1016/j.icarus.2011.01.004.

McEwen, A. S., et al. (2007), Mars Reconnaissance Orbiter's High Resolution Imaging Science Experiment (HiRISE), *J. Geophys. Res.*, *112*, E05S02, doi:10.1029/2005JE002605.

McGill, G. E. (1989), Buried topography of Utopia, Mars: Persistence of a giant impact depression, *J. Geophys. Res.*, *94*, 2753–2759, doi:10.1029/JB094iB03p02753.

McGovern, P. J., and M. M. Litherland (2011), Lithospheric stress and basaltic magma ascent on the Moon, with implications for large volcanic provinces and edifices, Lunar Planet. Sci., XLII, abstract #2587.

McGovern, P. J., K. Powell, G. Y. Kramer, and M. Litherland (2011), Stress-enhanced magma ascent at the margins of large impact basins in the solar system, AGU Fall Meeting 2011, abstract #P31E-1736.

Meresse, S., F. Costard, N. Mangold, P. Masson, G. Neukum, and the HRSC Co-I Team (2008), Formation and evolution of the chaotic terrains by subsidence and magmatism: Hydraotes Chaos, Mars, *Icarus*, *194*, 487–500, doi:10.1016/j.icarus.2007.10.023.

Michael, G. G., and G. Neukum (2010), Planetary surface dating from crater size-frequency distribution measurements: Partial resurfacing events and statistical age uncertainty, *Earth Planet. Sci. Lett.*, *294*, 223–229, doi:10.1016/j.epsl.2009.12.041.

Moore, H. J., J. J. Plaut, P. M. Schenk, and J. W. Head (1992), An unusual volcano on Venus, *J. Geophys. Res.*, *97*, 13,479–13,493, doi:10.1029/92JE00957.

Morrissey, M. M., B. Zimanowski, and K. Wohletz (1999), Phreatomagmatic Fragmentation, in *Encyclopedia of volcanoes*, edited by H. Sigurdsson, pp. 431–445, Academic Press, San Diego, California.

Mouginot, J., A. Pommerol, P. Beck, W. Kofman, and S. M. Clifford (2012), Dielectric map of the Martian northern hemisphere and the nature of plain filling materials, *Geophys. Res. Lett.*, *39*, L02202, doi:10.1029/2011GL050286.

Mueller, K., and M. Golombek (2004), Compressional structures on Mars, *Ann. Rev. Earth Planet. Sci.*, *32*, 435–464, doi:10.1146/annurev.earth.32.101802.120553.

Neish, C. D., R. D. Lorenz, and R. L. Kirk (2008), Radar topography of domes on planetary surfaces, *Icarus*, *196*, 552–564, doi:10.1016/j.icarus.2008.03.013.

Neumann, G. A., M. T. Zuber, M. A. Wieczorek, P. J. McGovern, F. G. Lemoine, and D. E. Smith (2004), Crustal structure of Mars from gravity and topography, *J. Geophys. Res.*, *109*, E08002, doi:10.1029/2004JE002262.

Nimmo, F. (2005), Tectonic consequences of Martian dichotomy modification by lower-crustal flow and erosion, *Geology*, *33*(7), 533–536, doi:10.1130/G21342.1.

Noguchi, R., and K. Kurita (2011), Double cone structure in Central Elysium Planitia, Mars, EPSC-DPS Joint Meeting 2011, abstract EPSC-DPS2011-415-1.

Ollier, C. D. (1967), Maars - their characteristics, varieties and definition, *Bull. Volcanol.*, *31*, 45–73, doi:10.1007/BF02597005.

de Pablo, M., and G. Caprarelli (2010), Possible Subglacial Volcanoes in Nepenthes Mensae, Eastern Hemisphere, Mars, LPSC, XLI, abstract #1584.

de Pablo, M. A., and A. Pacifici (2008), Geomorphological evidence of water level changes in Nepenthes Mensae, Mars, *Icarus*, *196*, 667–671, doi:10.1016/j.icarus.2008.04.005.

Pike, R. J. (1978), Volcanoes on the inner planets: Some preliminary comparisons of gross topography, Proc. Lunar Sci. Conf. IX, 3239–3273.

Plescia, J. B. (1990), Recent flood lavas in the Elysium region of Mars, *Icarus*, *88*, 465–490, doi:10.1016/0019-1035(90)90095-Q.

Plescia, J. B. (2003), Cerberus Fossae, Elysium, Mars: A source for lava and water, *Icarus*, *164*, 79–95, doi:10.1016/S0019-1035(03)00139-8.

Pondrelli, M., A. P. Rossi, G. G. Ori, S. van Gasselt, D. Praeg, and S. Ceramicola (2011), Mud volcanoes in the geologic record of Mars: The case of Firsoff Crater, *Earth Planet. Sci. Lett.*, *304*, 511–519, doi:10.1016/j.epsl.2011.02.027.

Porter, S. C. (1972), Distribution, morphology and size frequency of cinder cones on Mauna Kea volcano, Hawaii, *Geol. Soc. Am. Bull.*, *83*, 3607–3612, doi:10.1130/0016-7606(1972)83[3607:DMASFO]2.0.CO;2.

Rampey, M. L., K. A. Milam, H. Y. McSween, J. E. Moersch, and P. R. Christensen (2007), Identity and emplacement of domical structures in the western Arcadia Planitia, Mars, *J. Geophys. Res.*, *112*, E06011, doi:10.1029/2006JE002750.

Rice, J. W., W. Farrand, T. McCoy, M. Schmidt, and R. A. Yingst (2006), Origin of Home Plate, Columbia Hills, Mars: Hydrovolcanic hypothesis, Eos, Trans. – Am. Geophys. Union 87 (52) (Fall Meet. Suppl., abstract P41B-1274).

Richardson, J. A., J. E. Bleacher, and L. S. Glaze (2013), The volcanic history of Syria Planum, Mars, *J. Volcanol. Geotherm. Res.*, *252*, 1–13, doi:10.1016/j.jvolgeores.2012.11.007.

Robbins, S. J., G. Di Achille, and B. M. Hynek (2011), The volcanic history of Mars: High-resolution crater-based studies of the calderas of 20 volcanoes, *Icarus*, *211*, 1179–1203, doi:10.1016/j.icarus.2010.11.012.

Roberts, K. S., R. J. Davies, S. A. Stewart, and M. Tingay (2011), Structural control on mud volcano vent distributions: Example from Azerbaijan and Lusi, east Java, *J. Geol. Soc. Lond.*, *168*, 1013–1030, doi:10.1144/0016-76492010-158.

Rodriguez, S. R., W. Morales-Barrera, P. Layer, and E. González-Mercado (2010), A quaternary monogenetic volcanic field in the Xalapa region, eastern Trans-Mexican volcanic belt: Geology, distribution and morphology of the volcanic vents, *J. Volcanol. Geotherm. Res.*, *197*, 149–166, doi:10.1016/j.jvolgeores.2009.08.003.

Rotto, S., and K. L. Tanaka (1995), Geologic/geomorphic map of the Chryse Planitia region of Mars: US Geological Survey Misc, Invest. Series Map I-2441, scale 1:5,000,000.

Rubin, A. M. (1995), Propagation of magma-filled cracks, *Ann. Rev. Earth Planet. Sci.*, *23*, 287–336, doi:10.1146/annurev.ea.23.050195.001443.

Schmidt, M. E., T. J. McCoy, P. A. de Souza, W. H. Farrand, R. Gellert, G. Klingelhofer, S. W. Ruff, and N. Cabrol (2006), Geochemical evidence for the volcanic origin of Home Plate in the inner basin of the Columbia Hills, Gusev Crater. Eos, Trans. – Am. Geophys. Union 87 (52) (Fall Meet. Suppl., abstract P44A-07).

Scholten, F., K. Gwinner, T. Roatsch, K.-D. Matz, M. Wählisch, B. Giese, J. Oberst, R. Jaumann, G. Neukum, and the HRSC Co-Investigator Team (2005), Mars Express HRSC Data Processing - Methods and Operational Aspects, PE&RS, *71*, 1143–1152.

Schultz, R. A., and H. Frey (1990), A new survey of multiring impact basins on Mars, *J. Geophys. Res.*, *95*, 14,175–14,189, doi:10.1029/JB095iB09p14175.

Schultz, P. H., R. A. Schultz, and J. Rogers (1982), The structure and evolution of ancient impact basins on Mars, *J. Geophys. Res.*, *87*, 9803–9820, doi:10.1029/JB087iB12p09803.

Scott, D. H., and K. L. Tanaka (1986), Geologic map of the western equatorial region of Mars, US Geol. Surv. Geol. Inv. Ser. Map, I-1802-A.

Sheridan, M. F., and K. H. Wohletz (1983), Hydrovolcanism: Basic considerations and review, *J. Volcanol. Geotherm. Res.*, *17*, 1–29, doi:10.1016/0377-0273(83)90060-4.

Skinner, J. A., and A. Mazzini (2009), Martian mud volcanism: Terrestrial analogs and implications for formational scenarios, *Mar. Pet. Geol.*, *26*(9), 1866–1878, doi:10.1016/j.marpetgeo.2009.02.006.

Skinner, J. A., and K. L. Tanaka (2007), Evidence for and implications of sedimentary diapirism and mud volcanism in the southern Utopia highland-lowland boundary plain, Mars, *Icarus*, *186*, 41–59, doi:10.1016/j.icarus.2006.08.013.

Smith, P. H., et al. (2009), H_2O at the Phoenix landing site, *Science*, *325*, 58–61, doi:10.1126/science.1172339.

Spudis, P. D. (1993), *The Geology of Multi-Ring Impact Basins*, 263 pp., Cambridge Univ. Press, Cambridge, UK.

Tanaka, K. L., M. H. Carr, J. A. Skinner, M. S. Gilmore, and T. M. Hare (2003), Geology of the MER 2003 "Elysium" candidate landing site in southeastern Utopia Planitia, Mars, *J. Geophys. Res.*, *108*(E12), 8079, doi:10.1029/2003JE002054.

Tanaka, K. L., J. A. Skinner, and T. M. Hare (2005), Geologic map of the northern plains of Mars, scale 1:15,000,000, U.S. Geol. Surv. Sci. Invest., Map 2888, http://pubs.usgs.gov/sim/2005/2888/

Tibaldi, A. (1995), Morphology of pyroclastic cones and tectonics, *J. Geophys. Res.*, *100*, 24,521–24,535, doi:10.1029/95JB02250.

Tibaldi, A. (2005), Volcanism in compressional tectonic settings: Is it possible?, *Geophys. Res. Lett.*, *32*, L06309, doi:10.1029/2004GL021798.

Vespermann, D., and H.-U. Schmincke (2000), Scoria cones and tuff rings, in *Encyclopedia of volcanoes*, edited by H. Sigurdsson, pp. 683–694, Academic Press, San Diego, California.

Vincendon, M., F. Forget, and J. Mustard (2010), Water ice at low to midlatitudes on Mars, *J. Geophys. Res.*, *115*, E10001, doi:10.1029/2010JE003584.

Wadge, G., and A. Cross (1988), Quantitative methods for detecting aligned points: an application to the volcanic vents of the Michoacan–Guanajuato volcanic field, Mexico, *Geology*, *16*, 815–818, doi:10.1130/0091-7613(1988)016<0815:QMFDAP>2.3.CO;2.

Watters, T. R. (2003), Lithospheric flexure and the origin of the dichotomy boundary on Mars, *Geology*, *31*, 271–274, doi:10.1130/0091-7613(2003)031<0271:LFATOO>2.0.CO;2.

Watters, T. R., et al. (2007), Radar sounding of the Medusae Fossae Formation Mars: Equatorial ice or dry, low-density deposits?, *Science*, *318*, 1125–1128, doi:10.1126/science.1148112.

Werner, S. C. (2009), The global martian volcanic evolutionary history, *Icarus*, *201*, 44–68, doi:10.1016/j.icarus.2008.12.019.

White, J. D. L., and P.-S. Ross (2011), Maar-diatreme volcanoes: A review, *J. Volcanol. Geoth. Res.*, *201*, 1–29, doi:10.1016/j.jvolgeores.2011.01.010.

Wilson, L., and J. W. Head (1994), Review and analysis of volcanic eruption theory and relationships to observed landforms, *Rev. Geophys.*, *32*, 221–263, doi:10.1029/94RG01113.

Wilson, L., and J. W. Head (2004), Evidence for a massive phreatomagmatic eruption in the initial stages of formation of the Mangala Valles outflow channel, Mars, *Geophys. Res. Lett.*, *31*, L15701, doi:10.1029/2004GL020322.

Wilson, L., and P. J. Mouginis-Mark (2003a), Phreatomagmatic explosive origin of Hrad Vallis, Mars, *J. Geophys. Res.*, *108*(E8), 5082, doi:10.1029/2002JE001927.

Wilson, L., and P. J. Mouginis-Mark (2003b), Phreato-magmatic dike-cryosphere interactions as the origin of small ridges north of Olympus Mons, Mars, *Icarus*, *165*, 242–252, doi:10.1016/S0019-1035(03)00197-0.

Wohletz, K. H., and R. G. McQueen (1984a), Volcanic and stratospheric dust-like particles produced by experimental water-melt interactions, *Geology*, *12*, 591–594, doi:10.1130/0091-7613(1984)12<591:VASDPP>2.0.CO;2.

Wohletz, K. H., and R. G. McQueen (1984b), Experimental studies of hydromagmatic volcanism, in, *Geophysics Study Committee: Studies in Geophysics: Explosive volcanism: Inception. evolution, and hazards*, pp. 158–169, National Academy Press., Washington.

Wohletz, K. H., and M. F. Sheridan (1983), Hydrovolcanic explosions II. Evolution of basaltic tuff rings and tuff cones, *Am. J. Sci.*, *283*, 385–413, doi:10.2475/ajs.283.5.385.

Womer, M. B., R. Greeley, and J. S. King (1980), The geology of Split Butte – a maar of the south central Snake River Plain, Idaho, *Bull. Volcanol.*, *43*, 453–472, doi:10.1007/BF02597685.

Wood, C. A. (1979), Cinder cones on Earth, Moon and Mars, Lunar Planet. Sci. X, 1370–1372, abstract.

Wood, C. A. (1980), Morphometric evolution of cinder cones, *J. Volcanol. Geotherm. Res.*, *7*, 387–413, doi:10.1016/0377-0273(80)90040-2.

Wright, R., H. Garbeil, S. M. Baloga, and P. J. Mouginis-Mark (2006), An assessment of shuttle radar topography mission digital elevation data for studies of volcano morphology, *Remote Sens. Environ.*, *105*, 41–53, doi:10.1016/j.rse.2006.06.002.

Xiao, L., J. Huang, P. R. Christensen, R. Greeley, D. A. Williams, J. Zhao, and Q. He (2012), Ancient volcanism and its implication for thermal evolution of Mars, *Earth Planet. Sci. Lett.*, *323–324*, 9–18, doi:10.1016/j.epsl.2012.01.027.

Zuber, M. T., et al. (2000), Internal structure and early thermal evolution of Mars from Mars Global Surveyor topography and gravity, *Science*, *287*, 1788–1793.